



저작자표시-비영리-변경금지 2.0 대한민국

이용자는 아래의 조건을 따르는 경우에 한하여 자유롭게

- 이 저작물을 복제, 배포, 전송, 전시, 공연 및 방송할 수 있습니다.

다음과 같은 조건을 따라야 합니다:



저작자표시. 귀하는 원저작자를 표시하여야 합니다.



비영리. 귀하는 이 저작물을 영리 목적으로 이용할 수 없습니다.



변경금지. 귀하는 이 저작물을 개작, 변형 또는 가공할 수 없습니다.

- 귀하는, 이 저작물의 재이용이나 배포의 경우, 이 저작물에 적용된 이용허락조건을 명확하게 나타내어야 합니다.
- 저작권자로부터 별도의 허가를 받으면 이러한 조건들은 적용되지 않습니다.

저작권법에 따른 이용자의 권리는 위의 내용에 의하여 영향을 받지 않습니다.

이것은 [이용허락규약\(Legal Code\)](#)을 이해하기 쉽게 요약한 것입니다.

[Disclaimer](#)

February 2022

Doctor's Degree Thesis

**Development of Woven Structured and
Skin-attachable Nanogenerator for
Wearable Energy Harvesting**

Graduate School of Chosun University

Department of IT Fusion Technology

Jiwon Park

Development of Woven Structured and Skin-attachable Nanogenerator for Wearable Energy Harvesting

웨어러블 에너지 하베스팅을 위한
직물구조 및 신체부착형 나노제너레이터 개발

February 25, 2022

Graduate School of Chosun University

Department of IT Fusion Technology

Jiwon Park

Development of Woven Structured and Skin-attachable Nanogenerator for Wearable Energy Harvesting

Advisor: Prof. Youn Tae Kim

This thesis is submitted to The Graduate School of
Chosun University in partial fulfillment of the
requirements for the Doctor's degree.

October 2021

Graduate School of Chosun University

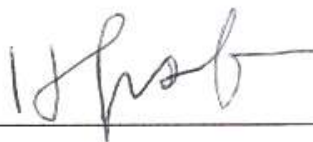
Department of IT Fusion Technology

Jiwon Park

This is to certify that the Doctor's Thesis of
Jiwon Park

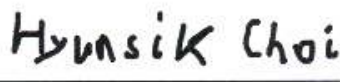
has been approved by the Examining Committee for the thesis
requirement for the Doctor's degree in IT Fusion Technology.

Committee Chairperson
Prof. Sung Bum Pan



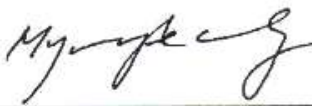
(Sign)

Committee Member
Prof. Hyun-Sik Choi




(Sign)

Committee Member
Prof. Myung-Ae Chung



(Sign)

Committee Member
Prof. Seon Jeong Kim



(Sign)

Committee Member
Prof. Youn Tae Kim



(Sign)

January 2022

Graduate School of Chosun University

Table of Contents

| | |
|--|-----------|
| Table of Contents | i |
| List of Figures | iv |
| List of Tables | ix |
| Acronyms | x |
| Abstract(Korean) | xi |
| | |
| I. Introduction | 1 |
| 1.1. Research background | 1 |
| 1.1.1. Wearable energy harvesting | 1 |
| 1.1.2. Triboelectric nanogenerators | 3 |
| 1.1.3. Outline of this dissertation | 6 |
| | |
| II. Flexible fiber and woven-structured triboelectric nanogenerator | 10 |
| 2.1. Experimental details | 10 |
| 2.1.1. Fabrication of the fiber-based TENG | 10 |
| 2.1.2. Fabrication of the woven-structured TENG | 12 |
| 2.1.3. Materials and measurement | 14 |
| 2.2. Results and discussion | 15 |
| 2.2.1. Working mechanism | 15 |
| 2.2.2. Output performance and stability | 17 |
| 2.2.3. Practical applications | 24 |

III. On-body-based triboelectric nanogenerator 27

3.1. Experimental details 27

 3.1.1. Fabrication of the on-body-based TENG and
 characterization 27

 3.1.2. Measurement 30

3.2. Results and discussion 31

 3.2.1. Working mechanism 31

 3.2.2. Output performance 33

 3.2.3. Stability and durability 36

 3.2.4. Practical applications 38

IV. TENG-based E-skin 41

4.1. Experimental details 41

 4.1.1. Fabrication of the patterned PDMS films 41

 4.1.2. Fabrication of electrode layer and TENG-based
 E-skin 43

 4.1.3. Characterization and measurement 45

4.2. Results and discussion 46

 4.2.1. Working mechanism 46

 4.2.2. Output performance and stability 48

 4.2.3. Comparison of the transparent and flexible TENGs 52

 4.2.4. Practical applications 53

V. Conclusion 55

References 57

List of Publications 67

Abstract(English) 73

Acknowledgement 75

List of Figures

| | | |
|------------|--|----|
| Figure 1.1 | Energy harvesting technologies for wearable devices. | 2 |
| Figure 1.2 | Triboelectric series. | 3 |
| Figure 1.3 | Working mechanism of TENG. (a) Initial state. (b) Contact electrification phenomenon. (c, d) Electrostatic induction and current generation. | 4 |
| Figure 1.4 | Types of TENG for wearable energy harvesting. | 5 |
| Figure 2.1 | (a) Schematic of the structure and two step manufacture process for the stretchable FTENG. (b) FESEM image of FTENG with a diameter and enlarged side image. (c) Photograph of the FTENG, released state and stretched state with 100% strain. | 11 |
| Figure 2.2 | (a) Schematic illustration of the WTENG; the figure on the right is the FTENG. (b) Electrical output depending on the number of conductive threads. (c) Photograph of the WTENG (45×45 mm ²). (d) Top-view FESEM image of the conductive thread. (e) Cross sectional view FESEM image of FTENG. (f) Photograph showing lighting of commercial LED connected to the conductive thread. | 13 |
| Figure 2.3 | (a-d) Schematic diagrams illustrating the working principles of the FTENG and WTENG under contact-separation motion. | 16 |
| Figure 2.4 | Electrical characteristics of the FTENG. (a) Output | |

| | | |
|-------------|--|----|
| | voltage and (b) current of the FTENG under a force of 1 kgf. | 17 |
| Figure 2.5 | Comparison of the electrical outputs according to the surface area of the WTENG: (a) $45 \times 45 \text{ mm}^2$, (b) $70 \times 35 \text{ mm}^2$, (c) $75 \times 75 \text{ mm}^2$ | 19 |
| Figure 2.6 | (a) Output voltage and current with different resistors as external loads. (b) Dependence of the output power on external load resistances. | 20 |
| Figure 2.7 | Mechanical durability test for the WTENG under 5000 cycles with the first and last 0.5 s waveforms enlarged. (a) Open-circuit voltage and (b) short-circuit current. | 22 |
| Figure 2.8 | (a) Photograph of the experimental setup for stretch-release cycles. (b) Output voltage and (c) current before and after stretching by 66.6% through 5000 cycles. | 23 |
| Figure 2.9 | (a) Circuit diagram of a full-wave bridge rectifier and charging curve for the capacitor. (b) The LED can be directly lit and is visible in bright environments. | 25 |
| Figure 2.10 | (a) The electrical watch was powered by the WTENG under the pushing mode. (b) Light of 82 white LEDs and visible in dark environment. (c) WTENG integrated in a shoe, harvesting energy from steps. | 26 |
| Figure 3.1 | (a) Schematic structure of on-body-based soft TENG. The inserts show the FESEM image, the EcoFlex thin | |

film surface, and the side of the Au-coated yarn.

(b) Summarized charge affinity for different triboelectric materials. (c) Data for resistance with different strains. (d) Photographs of soft TENG and (e) attached to a human hand with the electrode structure. 29

Figure 3.2 (a-d) Electricity generation mechanism of on-body-based soft TENG. 32

Figure 3.3 (a) Photograph of the experimental setup for the tensile strength test. (b) Load deformation curve. 34

Figure 3.4 (a, b) Electrical outputs under contact separation motion and (c, d) stretching motion. (e) Dependence of the output voltage and current on the external load resistance. (f) Output power per square meter of the on-body-based soft TENG. 35

Figure 3.5 (a) Photograph of experimental setup for pushing test. (b) Output voltage and (c) current from durability test under 2500 cycles. 36

Figure 3.6 (a) Photograph of experimental setup for tensile test. (b) Output voltage and (c) current before and after stretching under 2500 cycles. 37

Figure 3.7 (a) Circuit diagram of a full-wave bridge rectifier. (b) Electronic watch powered using a soft TENG. (c) Commercial LEDs directly lighted and visible in a dark environment. (d) Charging capability of on-skin-based soft TENG on a commercial capacitor of 1 μ F.

| | | |
|------------|---|----|
| | (e) Output voltages and (f) current of soft TENG mounted on different body parts. | 40 |
| Figure 4.1 | (a) Schematic of the fabrication process of patterned PDMS films and TENG-based E-skin. (b) FESEM images of PTFE-coated glass fabric tape and (c) patterned PDMS film, respectively. | 42 |
| Figure 4.2 | (a) Schematic of the structure of the conductive yarn. (b) FESEM image of the side of the conductive yarn. (c) FETEM images of the longitudinal section of TENG-based E-skin and conductive yarn electrode including (d) Ag-coated yarn and (e) polyesters. (f) Photograph of TENG-based E-skin. | 44 |
| Figure 4.3 | Schematic of the principle of the TENG-based E-skin in single-electrode mode. Current output under one cycle of contact and separation is shown in the figure. | 47 |
| Figure 4.4 | Stress-strain of the TENG-based E-skin. Inset is the resistance change of the conductive yarn with stretching strains. | 48 |
| Figure 4.5 | Electrical output performance including (a) Voc, (b) response and recovery time of Voc by the dashed black box, and (c) Isc. (d) The measured voltage, current, and (e) power density of the external load resistances. | 50 |
| Figure 4.6 | (a) Voc and (b) Isc from durability test under ~4500 cycles of contact-separation motions. (c) Photographs | |

of the cycling test setup with a pushing tester and (d) TENG-based E-skin at the initial state and 30% strain. 51

Figure 4.7 (a) Schematic of the equivalent circuit of a full-wave bridge rectifier. (b) Rectified voltage signal of a pulse signal input. (c) Capacitor charging at a frequency of 5 Hz. (d) Demonstration of powering an electronic watch by hand tapping the TENG-based E-skin. (e) Electrical output before and after bending the wrist. (f) Real-time arterial pulse waves. Inset is a photograph of a TENG-based E-skin on a wrist. 54

List of Tables

| | |
|--|----|
| Table 4.1 Comparison of energy harvesting and self-powered sensing characteristics of various transparent and flexible TENGs. | 52 |
|--|----|

Acronyms

| | |
|-------|--|
| PDMS | Polydimethylsiloxane |
| PTFE | Polytetrafluoroethylene |
| TENG | Triboelectric Nanogenerator |
| LED | Light Emitting Diode |
| AC | Alternating Current |
| DC | Direct Current |
| FTENG | Fiber-based Triboelectric Nanogenerator |
| WTENG | Woven-structured Triboelectric Nanogenerator |
| FESEM | Field Emission Scanning Electron Microscope |
| FETEM | Field Emission Transmission Electron Microscope |

요 약

웨어러블 에너지 하베스팅을 위한 직물구조 및 신체 부착형 나노제너레이터 개발

박지원

지도교수: 김윤태 교수, Ph. D.

조선대학교 대학원 IT융합학과

최근 스마트 의류, 전자 피부와 같은 착용형 시스템의 전원 공급 문제를 해결하기 위해 웨어러블 에너지 하베스팅 기술이 주목받고 있다. 본 논문에서는 사용자가 이질감 없이 착용하여 신체의 움직임으로부터 필요한 에너지를 수확하고 이를 다양한 분야에 응용 가능한 나노발전기를 제안하였다. 특히 웨어러블 에너지 하베스팅 소자의 핵심 요구 조건인 내구성과 유연성의 확보, 효율적인 발전 성능 향상을 위한 방법을 제시하였다. 이를 위해 본 논문에서는 파이버형, 직물 구조형, 신체 부착형, 전자 피부형 나노발전기를 제작하고 물리적, 전기적 특성을 측정하여 각 parameter의 영향을 분석하였다. 고분자 탄성중합체 및 전도성사의 복합화를 통해 신축성과 내구성을 동시에 확보하였고, 간단하고 효율적인 구조 방식으로 대전체 표면을 패터닝하여 전하 밀도를 증가시키고 소자의 발전 효율을 향상 시켰다. 제작된 소자는 100% 이상의 신축성, 5000회 동작 주기에 걸친 우수한 내구성, 최대 154 mW/m^2 의 전력을 생성하여 전자 기기를 동작시킬 수 있는 응용 가능성을 입증하였고 신체 움직임에 따른 에너지 수확뿐만 아니라 전자 피부형의 경우 일체형 압력 감지 센서로 응용하여 생체신호를 측정할 수 있었다. 개발된 나노발전기는 웨어러블 시스템에 전력 공급이 가능하고 전자 텍스타일, 유연전자소자, 휴먼-머신 인터페이스, 생체 모니터링 등의 응용 분야에 활용될 수 있을 것으로 기대된다.

I. Introduction

1.1. Research background

1.1.1. Wearable energy harvesting

Energy harvesting converts naturally occurring energy, such as sunlight, vibration, heat, and wind, into electricity. Because securing sustainable and eco-friendly energy is emerging as a necessity due to the depletion of raw materials and environmental pollution, energy harvesting technology is also expected to significantly impact future industrial development [1, 2]. In particular, as various wearable devices are developed, wearable energy harvesting technology for self-generation is gaining attention [3, 4]. Wearable energy harvesting converts the movement obtained from physical activity into power. This energy source is then used to operate a device [5]. The wearable energy harvesting generates electrical energy by using human body temperature and movement or by absorbing ambient electromagnetic waves. As shown in figure 1.1, wearable energy harvesting technology is largely divided into piezoelectric [6-8], thermoelectric [9, 10], and triboelectric [11-13] generations.

In piezoelectric generation, electrical energy is generated when mechanical deformation is applied to a piezoelectric material. Using this technology, energy is generated from small vibrations, such as heartbeat, pressure generated when people walk, or when the surface is bent [14, 15]. In addition, wearable energy harvesting can be applied to shoes, skin, textiles, and implantable devices.

In thermoelectric generation, thermal energy is converted into electrical energy and electrical energy into thermal energy based on the Seebeck and Peltier effects. Body temperature can be used to generate energy for wearable energy harvesting [16-18]. However, it must have high electrical conductivity and excellent flexibility, as it needs to absorb the maximum thermal energy from surfaces with considerable body movement.

In triboelectric generation, electricity that is generated on the contact surface by friction between two materials is collected. It is the most commonly used body movement-based wearable energy harvester owing to its advantages of high conversion efficiency and nanoscale design [19-21]. Therefore, a combination of materials that can generate more electricity with the same mechanical energy is important.

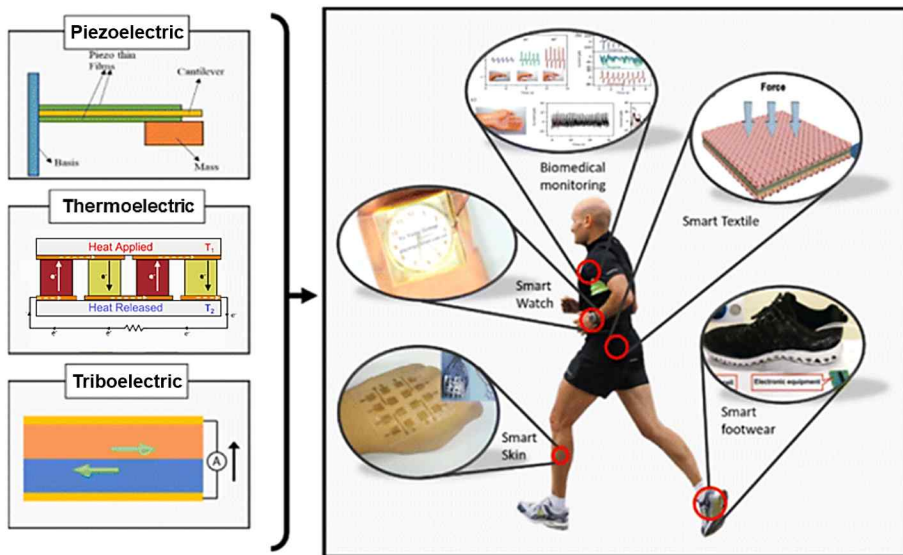


Figure 1.1. Energy harvesting technologies for wearable devices [22].

1.1.2. Triboelectric nanogenerator

A triboelectric nanogenerator (TENG) generates electrical energy based on contact electrification and electrostatic induction. Electrification refers to the phenomenon of electrical charging that occurs when two materials come into contact and separate. Surface charge density is a key factor in generating electrical energy using triboelectric materials [23–25]. As shown in figure 1.2, the triboelectric series determines the polarization of the surface triboelectric charges formed on the surface of the triboelectric material. The charges on the surface create a potential difference in the external circuit and induce the flow of electrons [26].

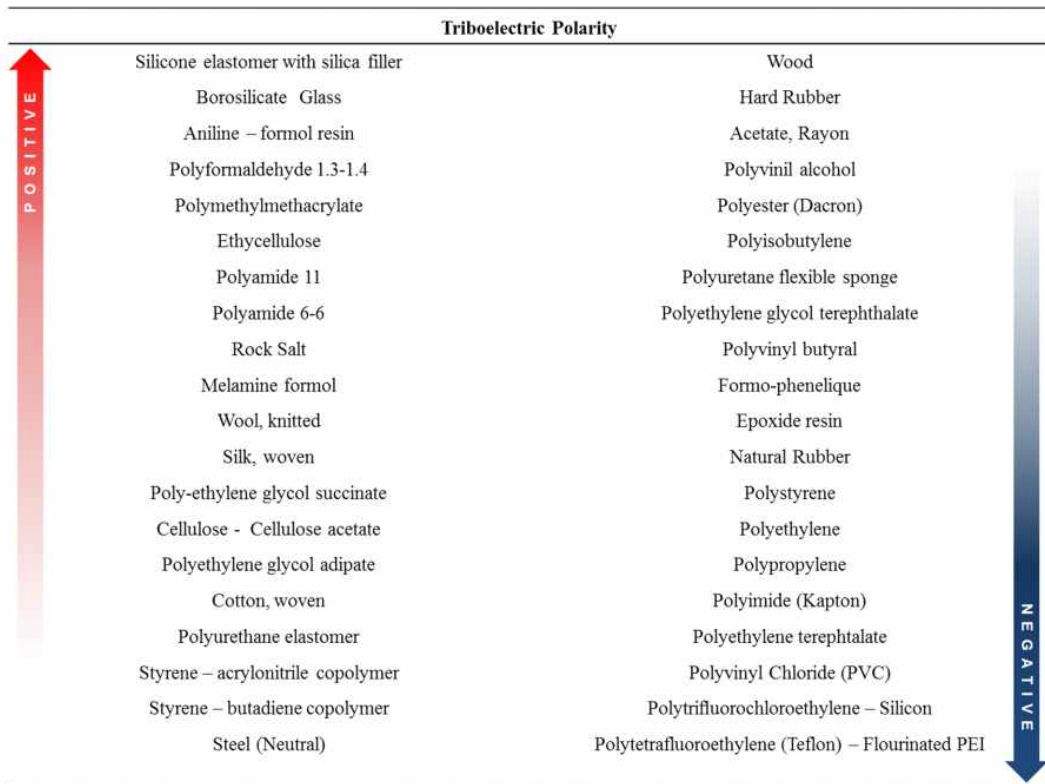


Figure 1.2. Triboelectric series [27].

As shown in figure 1.3, when two different materials come into contact, charge is transferred at the interface between the two materials. Furthermore, when a charge with opposite polarity is generated on the surface by friction between the two materials, the charge flows between the electrodes to maintain an electrostatic equilibrium by the relative movement of the triboelectric material [4, 28].

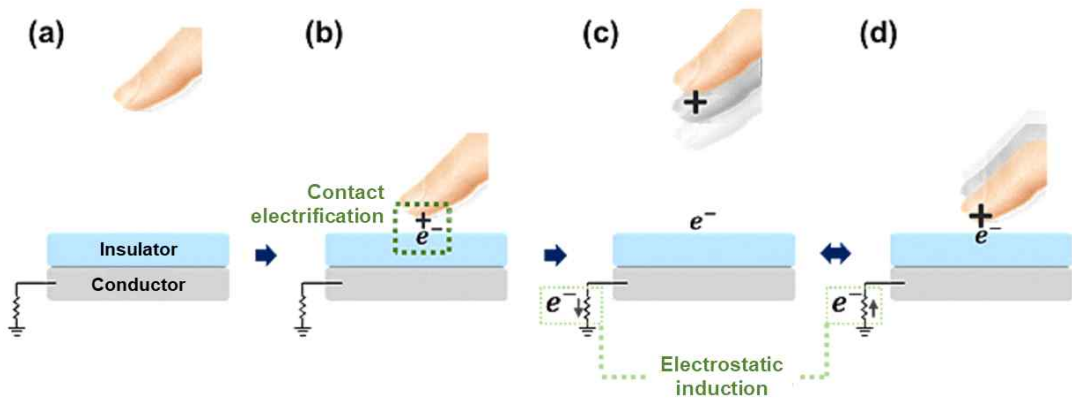


Figure 1.3. Working mechanism of TENG. (a) Initial state. (b) Contact electrification phenomenon. (c, d) Electrostatic induction and current generation.

TENG consists of two layers: an insulator and a conductor. Owing to this simple structure, TENG to be implemented as a wearable device. Recently, TENG has been increasingly used as a wearable device by utilizing transparent and stretchable materials for comfortable wearing (figure 1.4) [29, 30].



Figure 1.4. Types of TENG for wearable energy harvesting [29].

1.1.3. Outline of this dissertation

Worldwide, the research and development of wearable devices for medical, military, and user convenience is rapidly increasing. Currently, accessory-type products are the mainstream of wearable devices. However, the devices are expanding into clothing types and patches that can be directly attached to the skin, maximizing wearability, which is the strength of the fundamental technology [31-33]. Although wearable devices have evolved into a form that can be worn naturally on the body, the problem of continuous power supply remains the biggest technical challenge. To solve this problem, an energy-harvesting technology capable of self-generation of a device is attracting attention [34-36].

Energy harvesting technologies, such as piezoelectric, thermoelectric, and triboelectric harvesting technologies, can be integrated with wearable sensors [37, 38]. The piezoelectric energy-harvesting device converts the pressure difference, based on the human body movements, into electrical energy [39-41]. Existing piezoelectric materials are mostly inorganic-based oxides that exhibit high piezoelectric properties owing to their crystal structure. However, most of them are not bio-friendly and lack the flexibility required for applications in wearable types, resulting in low piezoelectric performance. For thermoelectric energy-harvesting devices that convert thermal energy into electrical energy using body temperature, research is underway on polymer-based elastic thermoelectric materials instead of metals that are difficult to deform [42-44]. However, soft organic materials are difficult to commercialize because of the disadvantage that the thermoelectric properties are easily lost when subjected to physical impact. Among them, triboelectric energy harvesting technology is attracting attention owing to its characteristics of a wider selection of materials, simpler mechanical structure, and higher flexibility than piezoelectric and thermoelectric generators [45-47].

A nanogenerator is a type of technology that converts mechanical energy as produced by small-scale physical change into electricity, and uses, and is a device that utilizes nanomaterials or has a nanoscale operating environment and nanoscale power performance. However, it is recently referred as a device that uses displacement current as the driving force for effectively converting mechanical energy into electric power and signal, disregarding if nanomaterials are used or not [48].

TENG generates electrical energy through contact potential and electrostatic induction [49]. An energy harvester that generates an appropriate electric power with a natural fit on the body has not been developed to a commercially available level. Therefore, it is most suitable to implement the wearable device as a textile or skin patch type to harvest the energy required from physical activity without causing any discomfort to the user and apply the device in various fields. Furthermore, flexible materials and improvements in output performance must be studied to apply TENG as a wearable device.

Recently, hydrogel has been used as a flexible and stretchable material for TENGs, but since it is an aqueous electrolyte solution, there are problems in that it causes dehydration and decreases mechanical elasticity and ionic conductivity [50, 51]. To improve the power generation of the TENG, research is being conducted on various methods, such as expanding the surface area to be charged, applying metal nanoparticles, and etching organic materials. However, this requires a complicated process and expensive equipment [50, 52]. In addition, most textile or skin patch-types TENGs require an additional metal wire to be connected to the electrode and the external electrical connection. Therefore, it is necessary to implement a durable and flexible material, an efficient method to improve output performance, and a TENG manufacturing technology that does not require an additional electrode connection.

In this study, fiber-type, woven-structured, body-attached, and E-skin-type TENGs were fabricated for wearable energy harvesting. This satisfies the need to be applied as a wearable type and presents a new direction that can contribute to the field of wearable electronics. As a nanogenerator, a micro/nano patterning material was used and the power performance in the nanoscale was analyzed. A polymer elastomer, which contains similar mechanical properties to human skin tissue, along with elasticity and flexibility, was used as a stretch material. Simultaneously, both elasticity and durability were secured by compounding conductive yarns. Furthermore, the charge density was increased by patterning the surface of the triboelectric material using a simple and efficient casting method, and an additional electrode connection was not required owing to the use of a conductive yarn as an electrode.

In the first chapter, we will discuss the highly stretchable fiber- and woven-structured TENGs. Previous fiber-based TENGs (FTENG) were difficult to fabricate into bendable or stretchable structures using metal electrodes. The FTENG proposed in this study was fabricated with a structure capable of maintaining elasticity and showed high stretchability and flexibility of more than 100%. The electrical output of 28 V and 0.56 μA was generated by the contact of the human skin with the electrification layer. In addition, the existing fiber-based woven-structured TENG (WTENG) was fabricated by crossing multiple fibers, but the fibers in this study can be fabricated into a two-dimensional woven structure by weaving one strand. The WTENG generated power of up to 34.4 $\mu\text{W}/\text{cm}^2$, and presented excellent durability and potential applications for electronic devices. It also showed the possibility of harvesting mechanical energy generated from body movements. This study can be applied to textile applications such as E-textiles and smart clothing, and is expected to be a new solution that can supply power to wearable or portable devices.

In the second chapter, we will discuss on-body-based TENG that can be attached to the human skin or curved parts of the body to generate energy from arbitrary motion. It presented an ultra-thin thickness of 200 μm and a stretchability of more than 100%, and generated a maximum power of 150 mW/m^2 . The practical application of charging storage devices to operate electronic devices was demonstrated, and energy could be harvested in various motions by attaching them to various parts of the body. This study is expected to be utilized as a thin and flexible soft power source that can replace the existing E-skin and bulk batteries, and can be used in the fields of flexible electronic devices, artificial muscles, and human-machine interfaces.

In the third chapter, we will discuss the E-skin-type TENG capable of energy harvesting and self-pressure sensing developed by fabricating micro-patterned PDMS films. The inverted micro-pattern was replicated on the surface of the PDMS film using a micro-knitted pattern of PTFE as a mold. Such surface patterning can promote the triboelectric effect by increasing the contact area and friction of the triboelectric material. As an energy harvester, it generates a power of 154 mW/m^2 and has also demonstrated a fast response time and excellent stability over 4500 pushing cycles. With a self-pressure sensor, it detects the wrist arterial pulse and shows the capability to monitor human physiological signals in real-time. This study is expected to be applicable to applications such as wearable power supplies, biological monitoring, and self-powered motion detection sensors.

II. Flexible fiber and woven-structured triboelectric nanogenerator

2.1. Experimental details

2.1.1. Fabrication of the fiber-based TENG

Figure 2.1(a) shows the schematic and manufacturing process of the fiber-based TENG (FTENG). An FTENG is a single-electrode tribo-electric generator with a core-shell structure consisting of silicone rubber and conductive thread. In the process of fabricating a FTENG, the liquid parts A and B of the silicone rubber are stirred in a 1:1 ratio, to produce a silicone rubber fiber. The bubbles generated during stirring are removed from the vacuum state and the liquid of the silicone rubber is injected into a cylindrical mold having an inner diameter of 0.8 mm, to be cured. The conductive threads are used as electrodes to transfer the induced charges. The conductive threads are connected to the motor and wound onto the silicone rubber fiber at a constant speed and spacing. Finally, the surface is dip coated with silicone rubber and dried at room temperature for approximately 3 h. Figure 2.1(b) shows a field emission scanning electron microscope (FESEM) photograph of an FTENG with a diameter of 1.2 mm, and its enlarged side image. This image shows the structure of the silicone rubber frame with the conductive thread coiled around it and a silicone rubber coating on the surface of the fiber. Figure 2.1(c) shows the initial state of the FTENG and its stretched state under 100% strain. Even when the length of the FTENG is increased, the electrical pathway along the conductive thread of the electrode remains constant.

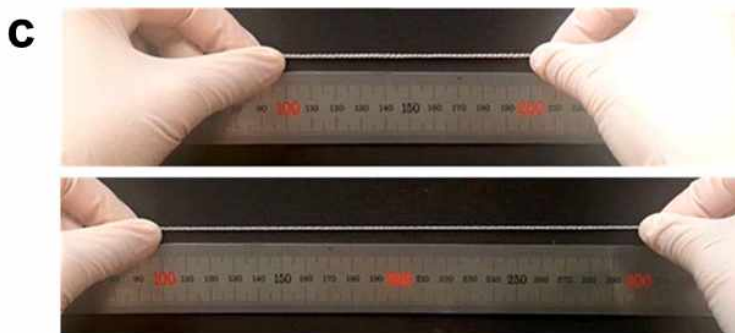
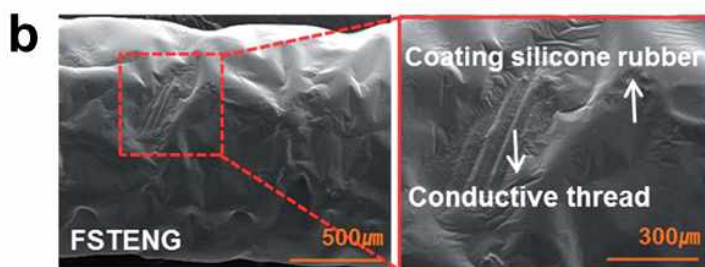
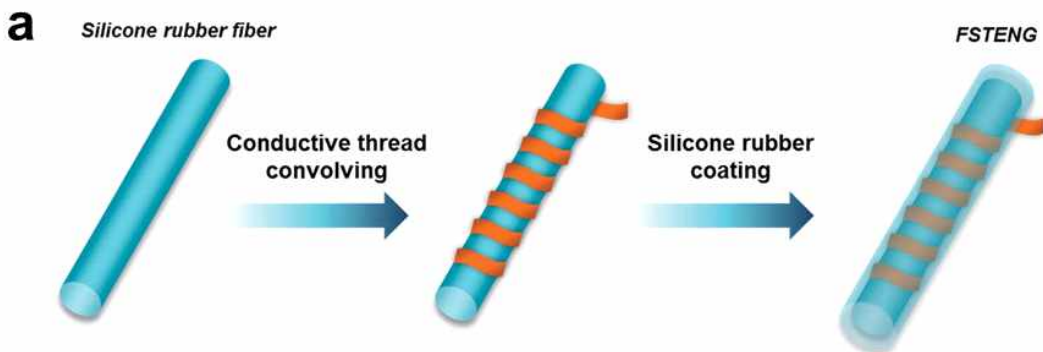


Figure 2.1. (a) Schematic of the structure and two step manufacture process for the stretchable FTENG. (b) FESEM image of FTENG with a diameter and enlarged side image. (c) Photograph of the FTENG, released state and stretched state with 100% strain.

2.1.2. Fabrication of the woven-structured TENG

As shown in figure 2.2(a), the woven-structured TENG (WTENG) consists of a single strand of a long FTENG. Prior to the weaving process, we compared the electrical output voltages according to the number of strands of the conductive thread, as shown in figure 2.2(b), to design the optimal FTENG. FTENGs consisting of one to six strands of the conductive thread showed different output values for an external force of 0.5 N. The highest output value was obtained with three strands of conductive thread. When more than four strands were used, the TENGs loosened under stretching conditions, resulting in damage to the coated silicone rubber and increasing the resistance. Therefore, we fabricated WTENGs with a $45 \times 45 \text{ mm}^2$ size, as shown in figure 2.2(c), based on the FTENG structure using three strands of conductive thread, through a weaving process using a weaving handloom. Figure 2.2(d) shows the FESEM image of the side of an conductive thread. The conductive threads are composed of multiple twisted conductive threads and polyester. Figure 2.2(e) shows the FESEM image of a FTENG cross-section fabricated with a radius of 0.6mm. The silicone rubber fiber and silicone rubber coated on the surface are shown in the image. The thickness of the silicone rubber layer on the surface is $100 \text{ }\mu\text{m}$. As shown in figure 2.2(f), a conductive thread was soldered on the breadboard to the anode and cathode of the LED. Using a DC supply, a voltage of 2 V was applied to illuminate the LED, demonstrating the excellent electrical conductivity and soldering interconnection characteristics of the conductive thread.

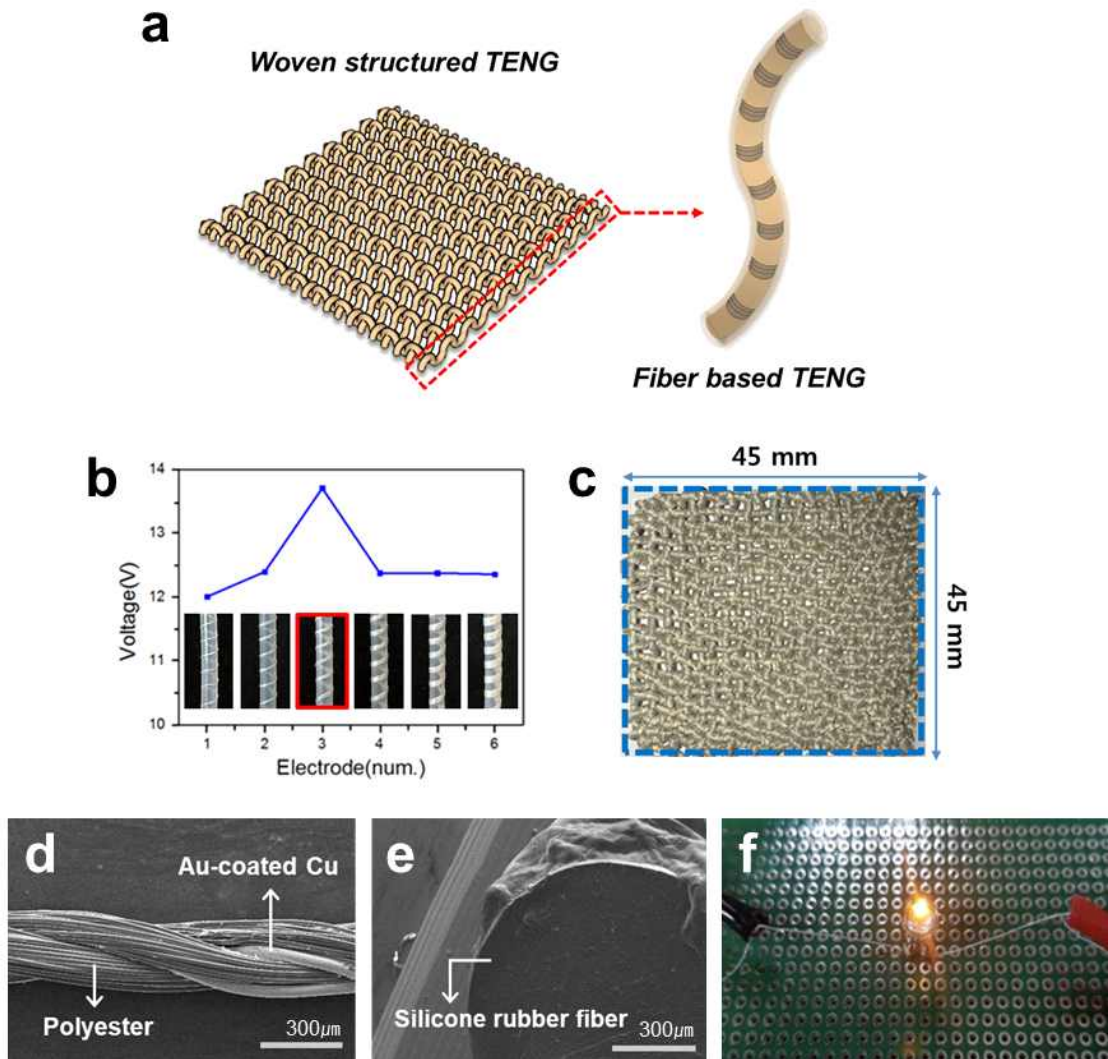


Figure 2.2. (a) Schematic illustration of the WTENG; the figure on the right is the FTENG. (b) Electrical output depending on the number of conductive threads. (c) Photograph of the WTENG ($45 \times 45 \text{ mm}^2$). (d) Top-view FESEM image of the conductive thread. (e) Cross sectional view FESEM image of FTENG. (f) Photograph showing lighting of commercial LED connected to the conductive thread.

2.1.3. Materials and measurement

The silicone rubber is used as a negative triboelectric material and has superior chemical stability, heat resistance, and abrasion resistance, when compared to the general organic rubber because of the inorganic properties of the main chain siloxane (Si-O) in the molecular structure. The silicone rubber is also used as a dielectric and encapsulating material for FTENG and WTENG because of its excellent flexibility, stretchability, biocompatibility, mechanical properties, strong resistance to sweat and water, and high electron affinity.

The conductive thread, which provides high conductivity and electrical stability, is composed of silver-coated copper and polyester and has an average resistance of 0.049 Ω /cm for a diameter of 300 μm . It exhibits higher mechanical durability, flexibility, and electrical conductivity, compared to other threads coated with metal [53-57].

The open-circuit voltage was measured using an MSO9104A digital oscilloscope, whereas the short-circuit current was measured using a B2911A precision source/measurement device. The applied force was measured using a CI-10W digital indicator. A JIPT-100 pushing tester was employed to drive the TENGs under a cyclic compression force, whereas the MCT-2150 tensile tester was employed to test the stability employing strain. Applications performance of the TENG was directly measured using practical hand tapping.

2.2. Results and discussion

2.2.1. Working mechanism

A TENG has various modes depending on the contact method of the device and the position of the electrode [58]. The single-electrode mode uses electrodes only on one material, out of the two different materials that are in contact. This mode has a structure that changes free-moving motion into electric current, and generates current in the course of maintaining the balance of electric charges, through the movement of electrons from the electrodes according to the contact or separation of the charged substances. This single-electrode mode has the advantage that the movements of the other materials are not limited.

As shown in the mechanism in figure 2.3, the FTENG and WTENG generate electric current while balancing the charge, by the movement of electrons from the electrode due to the friction between silicone rubber and the skin. According to the triboelectric series, silicone rubber has a negative characteristic with a high electron affinity, but skin shows a positive characteristic with a low electron affinity. As shown in figure 2.3(a), when skin and silicone rubber are in contact, the skin is positively charged and the silicone rubber is negatively charged. Thus, the silicone rubber generates a negative charge Q , and by induction of static electricity and preservation of charge, the conductive thread of the TENG electrode and the skin generate positive charges Q_1 and Q_2 , respectively. Therefore, since $Q = -(Q_1 + Q_2)$, the negative charge Q on the TENG is considered to create an electric field. As shown in figure 2.3(b), when the two materials are separated, a potential difference occurs and electrons move from the electrode to balance the triboelectric potential. As shown in figure 2.3(c), when the two materials are maximally separated, they enter electrostatic equilibrium states in which

electrons do not move. Finally, as shown in figure 2.3(d), when the two materials come into contact again, the electrostatic equilibrium collapses and the amount of charge moving from the electrode decreases. That is, Q_1 increases and Q_2 decreases, generating an electric current instantaneously. Hence, the TENG is a single-electrode structure that converts motion into electric current, is independent of the kind of motion, and generates alternating current (AC) through a continuous contact-separation process.

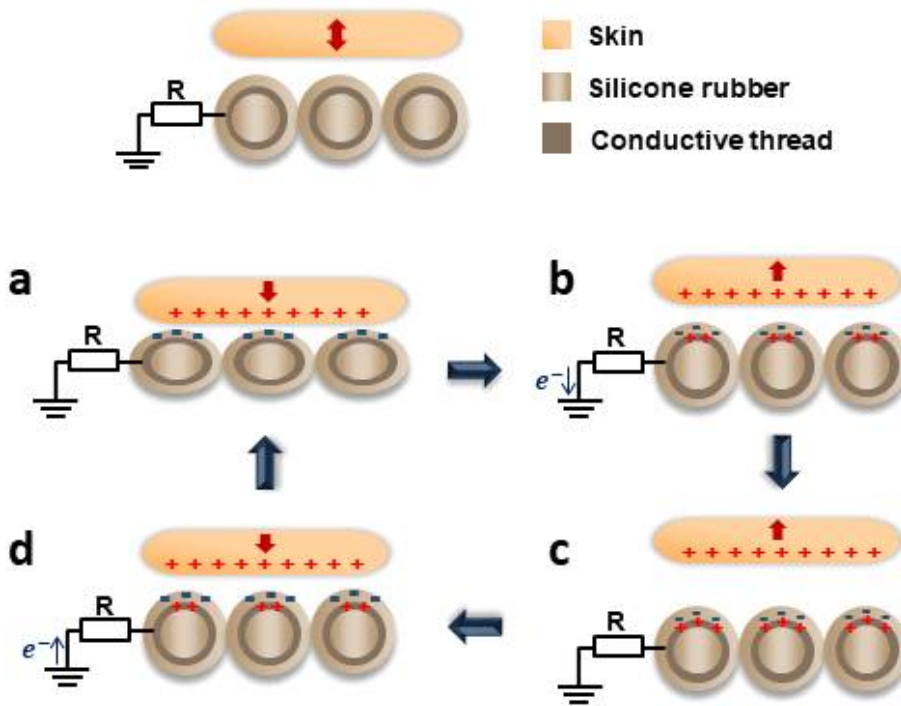


Figure 2.3. (a-d) Schematic diagrams illustrating the working principles of the FTENG and WTENG under contact-separation motion.

2.2.2. Output performance and stability

In FTENG, silicone rubber is a triboelectric layer that generates electrical output through friction with human skin. The electrical characteristics are analyzed by bringing an FTENG 8.5 cm in length and 1.2 mm in diameter in contact with human skin. When the skin and FTENG are in contact with a force of 1 kgf, the instantaneous voltage and current signals can be measured. The maximum output voltage and current are 28 V and 0.56 μA , as shown in figure 2.4(a) and (b).

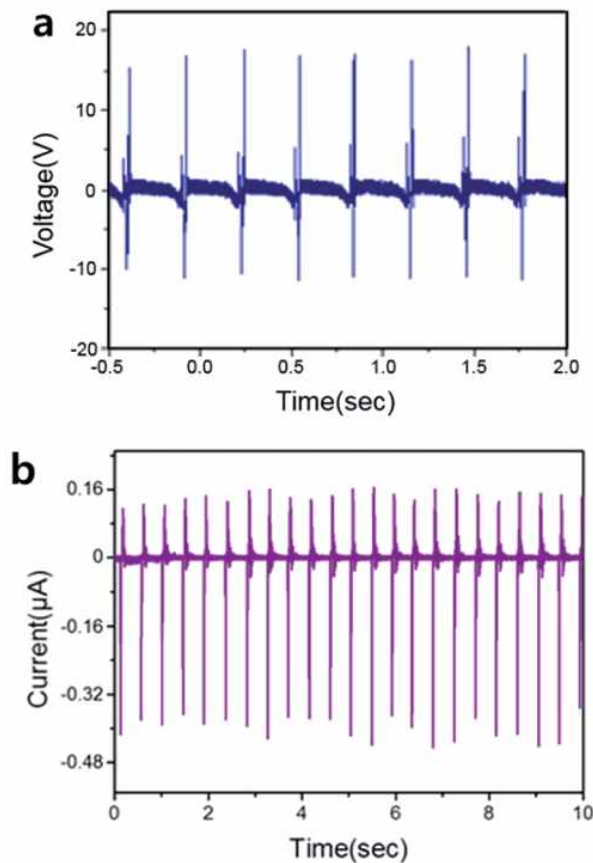


Figure 2.4. Electrical characteristics of the FTENG. (a) Output voltage and (b) current of the FTENG under a force of 1 kgf.

The proposed WTENG can be weaved in various sizes and shapes by using a weaving handloom. The WTENG was fabricated in various sizes, and experiments were conducted to analyze the electrical output characteristics on applying a repetitive external force. Figure 2.5 shows the output voltage and current signals generated from the WTENG by skin friction for an applied force of 1 kgf. As shown in figure 2.5(a), an output voltage of 42 V and current of 5 μ A was generated by a $45 \times 45 \text{ mm}^2$ WTENG. In the same experimental environment, as shown in figure 2.5(b), an WTENG with $70 \times 35 \text{ mm}^2$ size produced the maximum electrical output of 53 V and 15 μ A; an output of 72 V and 18 μ A was measured from the WTENG of size $75 \times 75 \text{ mm}^2$ (figure 2.5(c)). From these results, it can be inferred that the efficiency of electric power generation is improved as the size of the WTENG increases; however, this improvement is nonlinear. This may be because of a characteristic of triboelectricity, which induces saturation above a certain level of force. Therefore, it is important to select an optimal TENG size that offers efficient electrical output when a constant force is applied.

In addition, to investigate the effective electric power, WTENG was connected to electrical resistors and the electrical output was measured. As the resistance increased, the output voltage increased and was saturated at the open-circuit voltage when the resistance was infinitely large. Conversely, the output current decreased as the resistance increased (figure 2.6(a)). As a result, the output power showed a maximum value (about $34.4 \mu\text{W}/\text{cm}^2$), calculated from the equation ($W = V_{\text{peak}}^2/R$), at an external resistance of 1 M Ω (figure 2.6(b)).

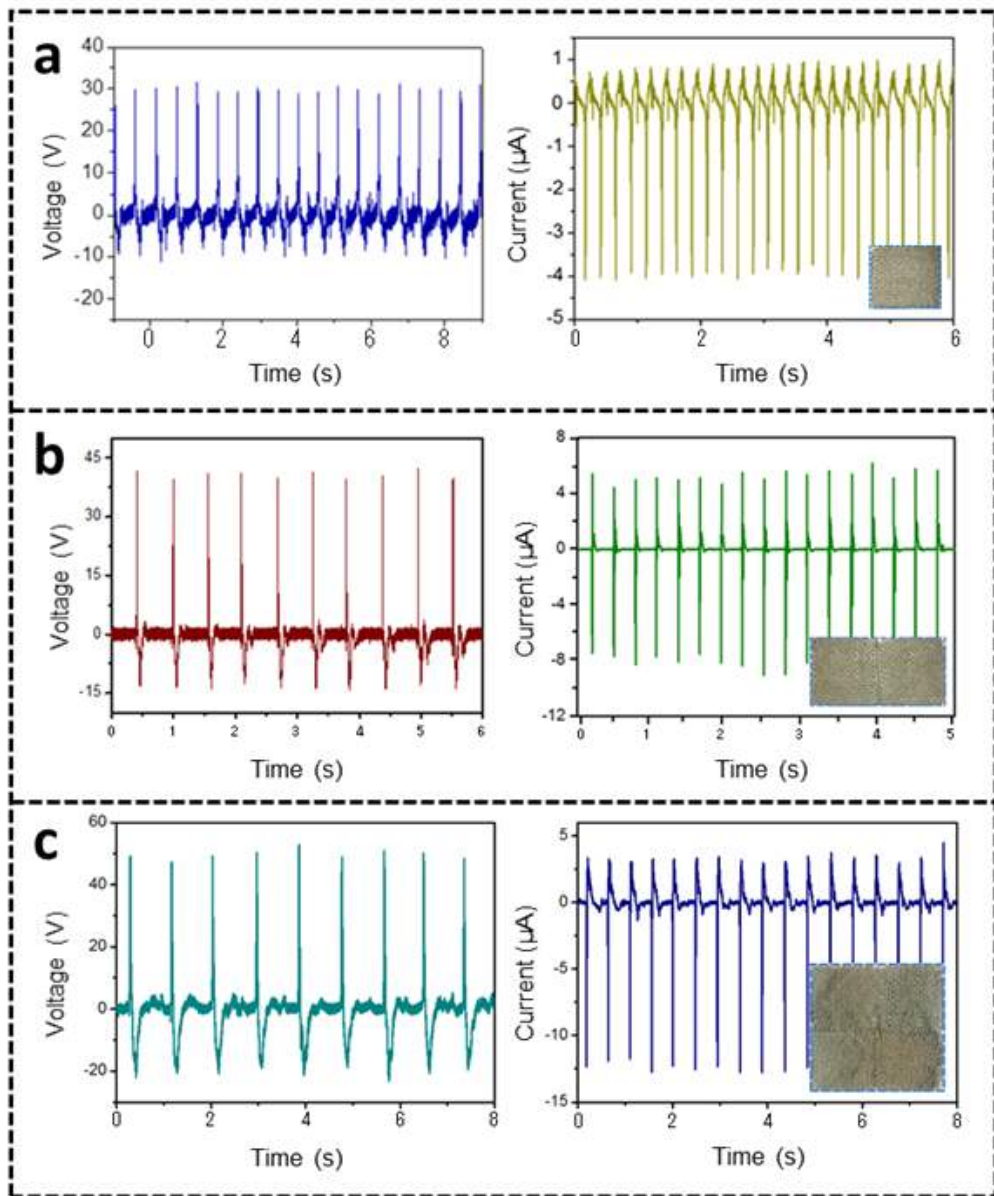


Figure 2.5. Comparison of the electrical outputs according to the surface area of the WTENG: (a) $45 \times 45 \text{ mm}^2$, (b) $70 \times 35 \text{ mm}^2$, (c) $75 \times 75 \text{ mm}^2$.

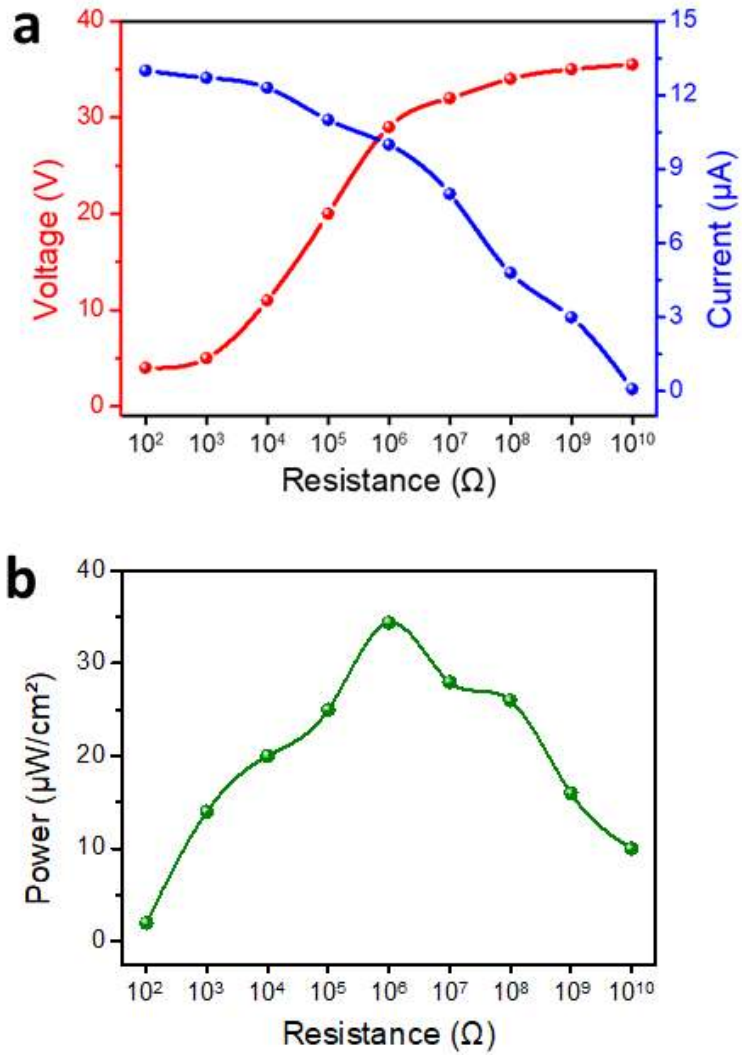


Figure 2.6. (a) Output voltage and current with different resistors as external loads. (b) Dependence of the output power on external load resistances.

Durability and stability are important parameters for the TENG as well as electrical energy generation. When a repetitive external force was applied, the WTENG exhibited a stable output performance. The contact area of the pushing tester applying the external force to the WTENG was $36\pi \text{ mm}^2$. As shown in figure 2.7(a), an output voltage was generated during 5,000 pushing cycles with a force of approximately 0.6 kgf. When comparing the output voltages of the initial state and the state after 5,000 pushing cycles, a constant value was confirmed, without distortion. Likewise, the current signal generated during 5,000 pushing cycles in the same experimental environment is shown in figure 2.7(b). Hence, the WTENG is of practical value as a reliable energy harvester since there is no reduction in the electrical output after an external force is applied.

In addition, to verify the flexibility of the WTENG, a triboelectric output test was conducted before and after specific stretch-release cycles by using a tensile tester (figure 2.8(a)). Figures 2.8(b) and (c) show the comparisons of the voltages and currents of the WTENG before and after the stretching tests wherein it was stretched by 66.6% through 5,000 cycles. The results show that a stable triboelectric performance was obtained. Thus, it can be concluded that the WTENG shows outstanding flexibility without degrading the electrical output.

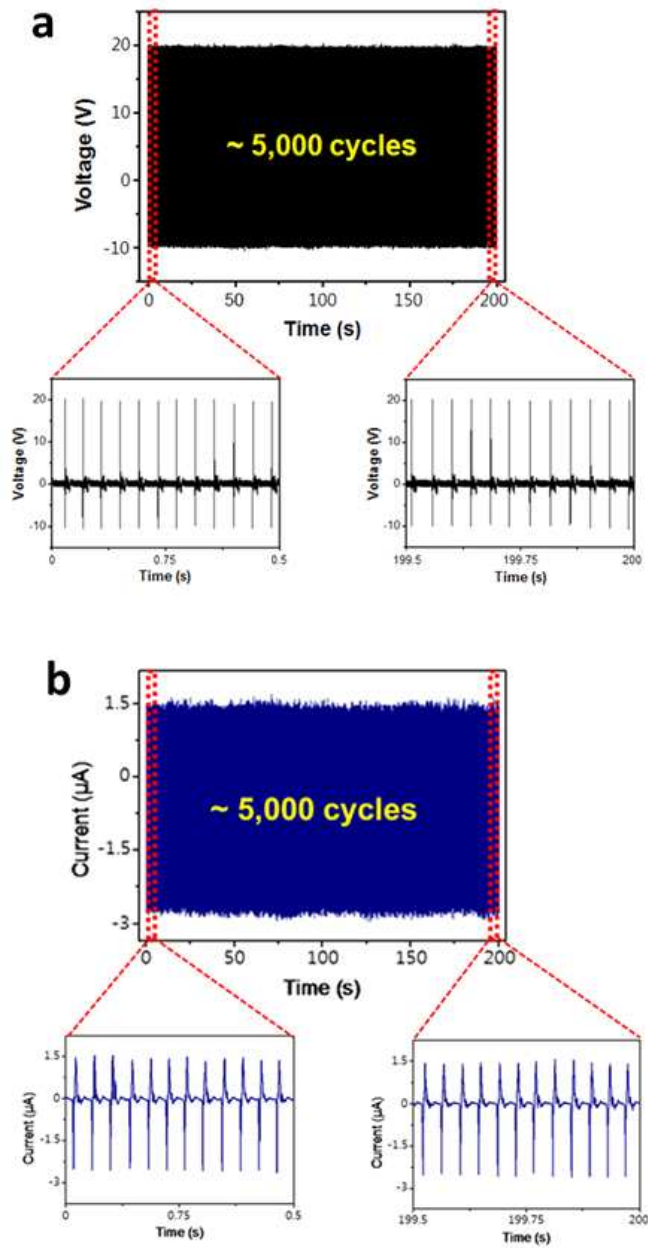


Figure 2.7. Mechanical durability test for the WTENG under 5000 cycles with the first and last 0.5 s waveforms enlarged. (a) Open-circuit voltage and (b) short-circuit current.

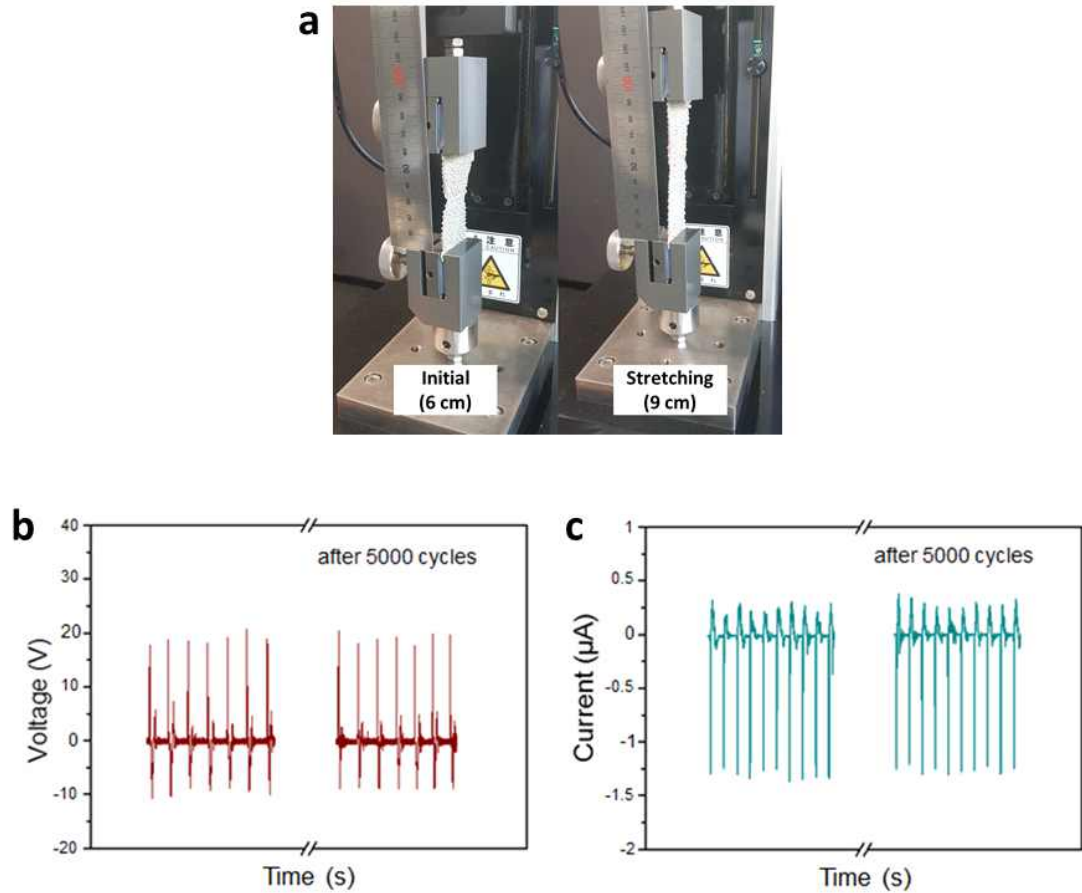


Figure 2.8. (a) Photograph of the experimental setup for stretch-release cycles. (b) Output voltage and (c) current before and after stretching by 66.6% through 5000 cycles.

2.2.3. Practical applications

We now demonstrate the potential applications for harvesting and substantially utilizing the electrical energy generated from WTENGs. As shown in figure 2.9(a), a capacitor was connected to the rectifier circuit and the charge level was measured as the voltage. The capacitor accumulated the charge until the positive and negative charges were equal to the voltages supplied externally. Since the WTENG generates AC, a bridge rectifier circuit was used. An external force was applied to an WTENG with size $70 \times 35 \text{ mm}^2$, which produced the highest power per unit area, and a $1 \text{ }\mu\text{F}$ capacitor was charged to 1.2 V for 25 s . According to the formula $Q = CV$, the amount of charge stored in the $1 \text{ }\mu\text{F}$ capacitor over 25 s is approximately $1.2 \text{ }\mu\text{C}$. As shown in figure 2.9(b), using the accumulated charge, a commercial LED was lit up.

In addition, the possibility of driving electronic devices was confirmed by connecting an electrical watch to an WTENG of size $70 \times 75 \text{ mm}^2$ and a rectifier circuit. In order to drive the electrical watch for a long time, a $1 \text{ }\mu\text{F}$ capacitor was connected to the circuit to increase charge capacity. As shown in figure 2.10(a), the electrical watch was driven continuously through contact with skin, under a pushing motion. To verify the LED operation, we use a white commercial LED that requires a minimum voltage of 1.8 V and a current of 100 mA . Since the WTENG can generate enough electrical output, 82 LEDs are connected in series and driven. Figure 2.10(b) shows the letters 'IFRC' formed by LED lights that are lit by contacting the human skin with an WTENG. In another application, the WTENG was attached to the heel of a shoe in order to convert the mechanical energy generated from the movement of the human body into electric energy. As shown in figure 2.10(c), a signal of instantaneous power was generated by the contact of the heel and the WTENG during a step. The WTENG can be applied to active sensors that calculate the

number of steps, gait correction shoes, portable power sources, etc., and can be further extended to other applications. It has been proven that the WTENG successfully outputs electrical energy as a self-powered device, and that it can be used as a promising power source for wearable devices.

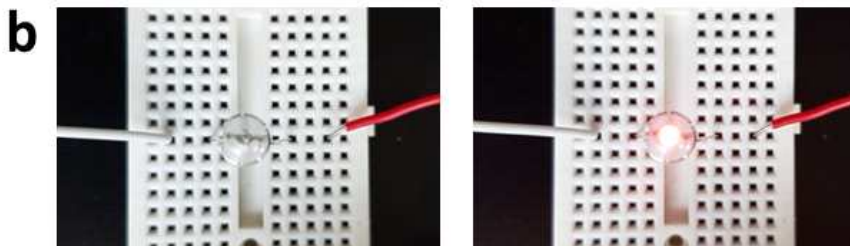
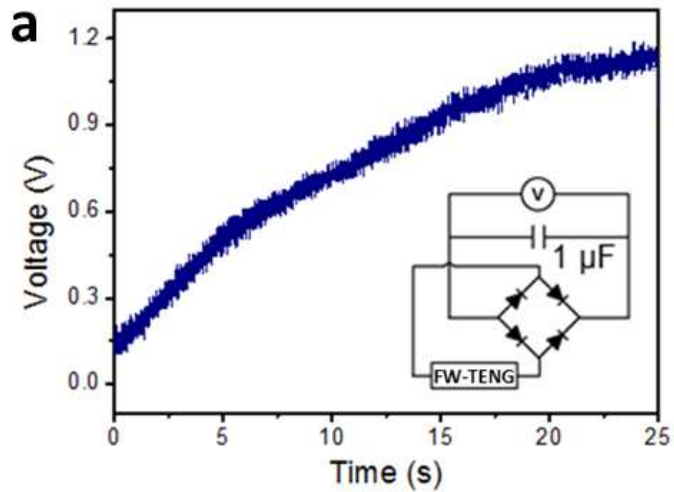


Figure 2.9. (a) Circuit diagram of a full-wave bridge rectifier and charging curve for the capacitor. (b) The LED can be directly lit and is visible in bright environments.

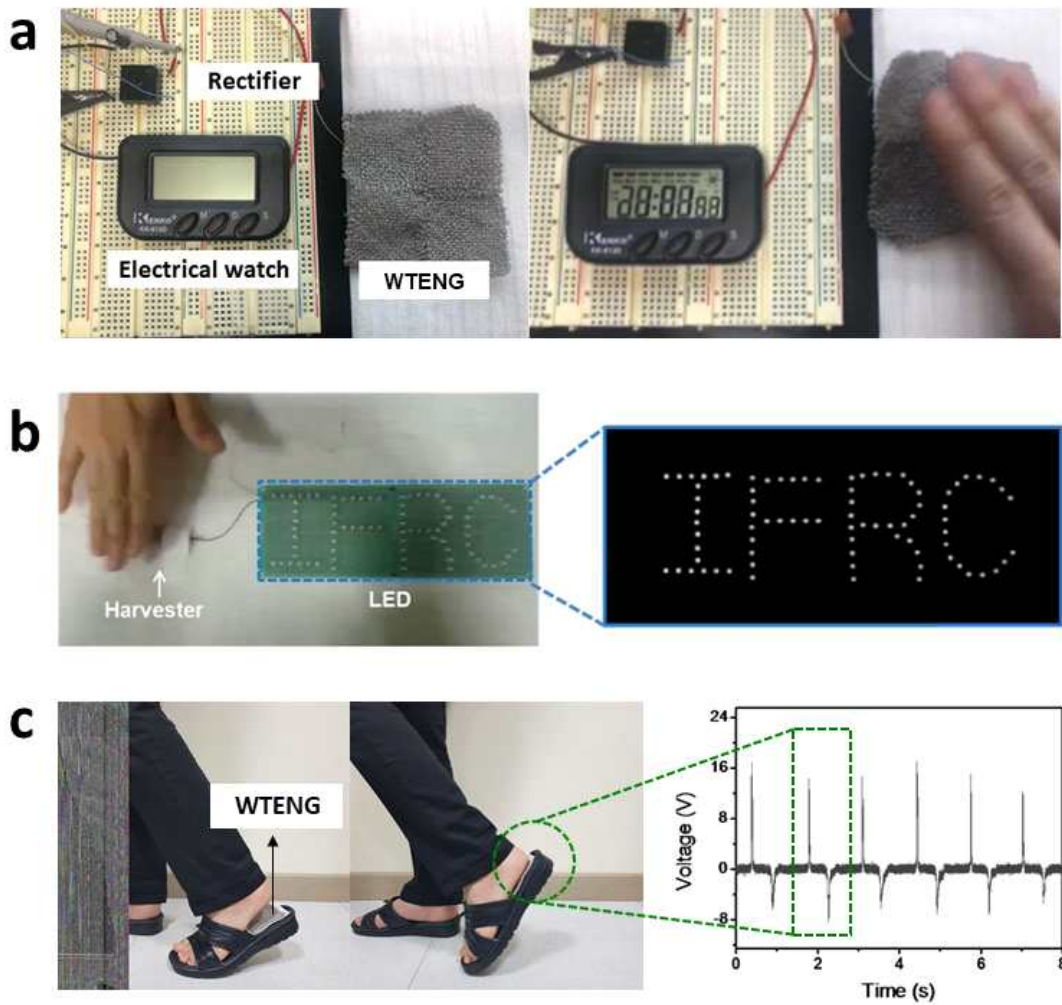


Figure 2.10. (a) The electrical watch was powered by the WTENG under the pushing mode. (b) Light of 82 white LEDs and visible in dark environment. (c) WTENG integrated in a shoe, harvesting energy from steps.

III. On-body-based triboelectric nanogenerator

3.1. Experimental details

3.1.1. Fabrication of the on-body-based TENG and characterization

Figure 3.1(a) shows a three-dimensional schematic diagram of the designed on-body-based soft TENG. The electrode formed on the dielectric surface in a serpentine shape was placed in the center, and the upper and lower surfaces had a sandwich structure composed of the EcoFlex thin film. EcoFlex (silicone rubber), a silicone-based elastic polymer material, is used as a negative triboelectric material and has a wide range of applications, such as being used as a stretchable electronic substrate or a flexible device because it is flexible, has excellent elasticity, and is harmless to the human body. For the EcoFlex mixture on the surface, a monomer and a curing agent were stirred at a ratio of 1:1. The mixture was polymerized for 3 h to prepare a solution of an elastic polymer. The thickness of the glass plate was measured by casting the EcoFlex solution horizontally, vertically, and vertically in air to obtain the best thin film thickness. From the findings, it was cured vertically in air to a thin uniform thickness of 200 μm . The bubbles generated during this process were stored in a vacuum and removed. Figure 3.1(a) shows the FESEM image of the EcoFlex thin film surface and the side of the Au-coated yarn, a conductive material used as the electrode. A weaving loom was used to form a serpentine shape of the Au-coated yarn at a spacing of 0.7 cm to form an electrode layer on the thin film surface. The distance between the pins of the weaving loom is 0.7 cm. The output performance of the TENG decreases as the width of the pattern increases. This occurs because the amount of charge transfer per unit area of the electrode is proportional. The Au-coated yarn consisted of three strands of metal filaments (40 μm diameter of Au-coated Cu) and polyester filaments (75 deniers with 36 filaments), exhibiting a resistance of

0.037 Ω/cm and a higher electrical conductivity than other conductive yarns. An electrode layer was formed on the thin film and fixed by spraying polytetrafluoroethylene (PTFE). PTFE helps maintain the flexibility of the EcoFlex thin film without affecting the thickness of the TENG as it is sparsely sprayed on the thin film. Finally, a thin film was placed on top before the PTFE was cured. As shown in figure 3.1(b), PTFE and EcoFlex has a high negative charge affinity (-190 nC/J and -72 nC/J), so it can increase the output by generating a high amount of frictional charge in materials with desirable properties [58, 59]. The resistance value was measured when unidirectional deformation was determined using a digital multimeter to observe the electrical conductivity changes in the electrode based on the TENG deformation. As shown in figure 3.1(c), when a strain up to 155% was applied, the resistance value linearly increased from its initial resistance of 9.7 k Ω to small width. However, when the strain exceeded the threshold, the resistance significantly increased, as the electrode was disconnected. In other words, it is possible to maintain adequate output performance of the device within a variation of a section in which the conductivity of the electrode changes to a low value based on the threshold value. The fabricated on-body-based soft TENG consisted of an optically transparent device with a size of $50 \times 40 \text{ mm}^2$ and a device attached to the back of the hand, as shown in figures 3.1(d) and (e). It was easy to attach TENG to the skin, and the device was flexible such that it could sense the movement of the human body and harvest energy.

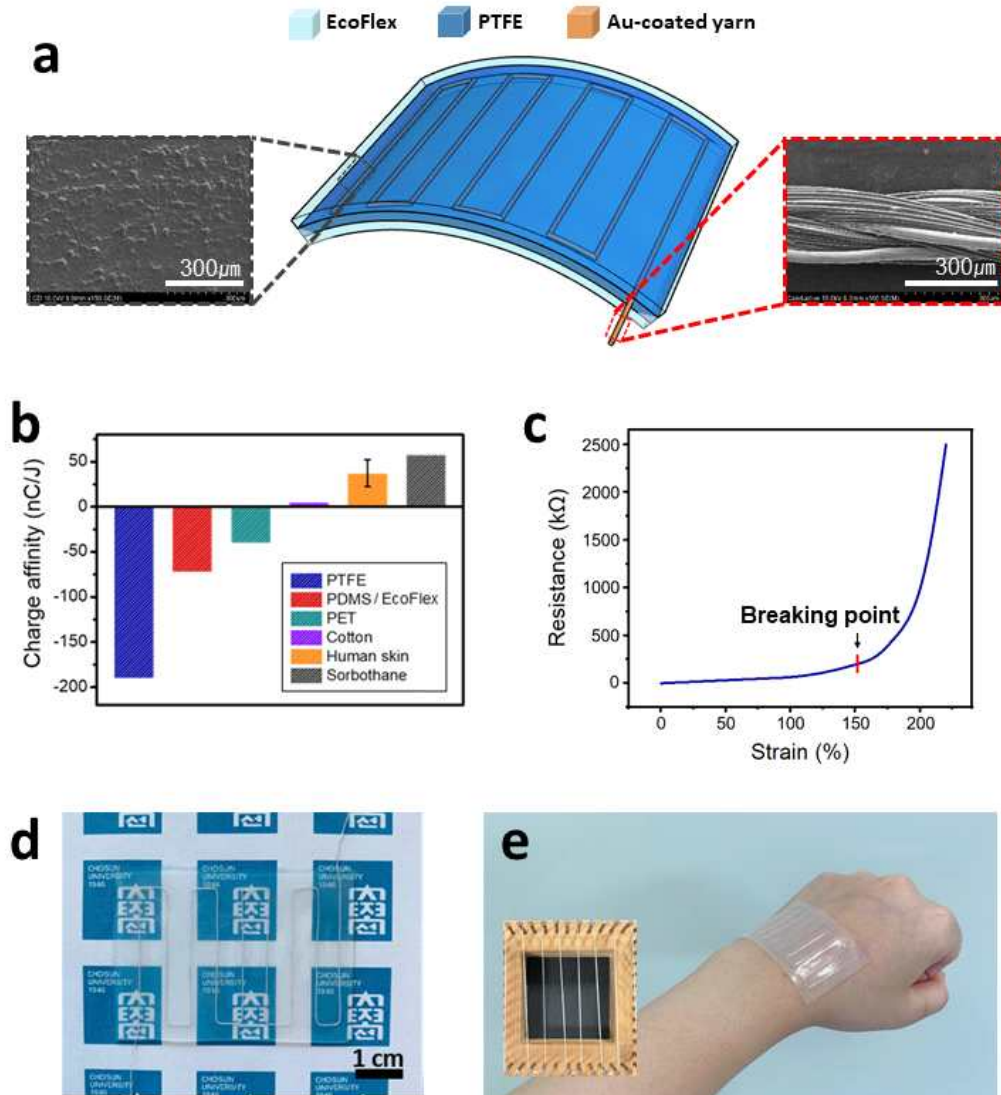


Figure 3.1. (a) Schematic structure of on-body-based soft TENG. The inserts show the FESEM image, the EcoFlex thin film surface, and the side of the Au-coated yarn. (b) Summarized charge affinity for different triboelectric materials. (c) Data for resistance with different strains. (d) Photographs of soft TENG and (e) attached to a human hand with the electrode structure.

3.1.2. Measurement

The open-circuit voltage was measured using an MSO9104A digital oscilloscope, whereas the short-circuit current was measured using a B2911A precision source/measurement device. The resistance value was measured using a DT-9205A digital multimeter, and the applied force was measured using a CI-10W digital indicator. A JIPT-100 pushing tester was employed to drive the TENGs under a cyclic compression force, whereas the MCT-2150 tensile tester was employed to measure the tensile strength and test the stability employing strain. The electrical output performance of the body-attachable TENG was directly measured using practical hand tapping and human body movements.

3.2. Results and discussion

3.2.1. Working mechanism

Figure 3.2 shows the cross-section of the on-body-based soft TENG and describes the principle of energy generation. The triboelectric output was generated by the flow of charged electric charges collected through the electrostatic induction phenomenon to the electrode by positive and negative electrical friction. As depicted in figure 3.2(a), the contact between EcoFlex and the skin created charges of opposite polarity on each surface because of the electron affinity from the triboelectric series. That is, based on the triboelectric effect and electrostatic induction, the EcoFlex on the TENG surface accumulated negative charges, while positive charges were accumulated on the skin. The higher the difference in the electron affinity of the triboelectric materials, the more charges that were accumulated. As shown in figure 3.2(b), when the surface was separated, a potential drop was established. During the process of balancing the potential, a transient charge flowed to the Au-coated yarn electrode, which generated a current pulse. According to a theoretical study on TENG [60], the output current is related to the charge transferred from the material surface and can be expressed as follows:

$$I(t) = \frac{\partial \Delta Q(t)}{\partial t}$$

where $\Delta Q(t)$ is the transferred charge. As shown in figure 3.2(c), electrostatic equilibrium was achieved when the interacting surface of the TENG and skin were separated by the maximum distance, and electrons accumulated on the electrode. Finally, as shown in figure 3.2(d), when the skin returned, the electrostatic equilibrium collapsed, and the charge moved in the opposite direction, creating a reverse current pulse. During each cycle of the mechanism, both positive and negative peak currents were generated, and

energy output could be generated through a continuous contact separation process. In addition, as a single electrode structure that converted free-moving motion into electric current, there was an advantage of the motion not being restricted.

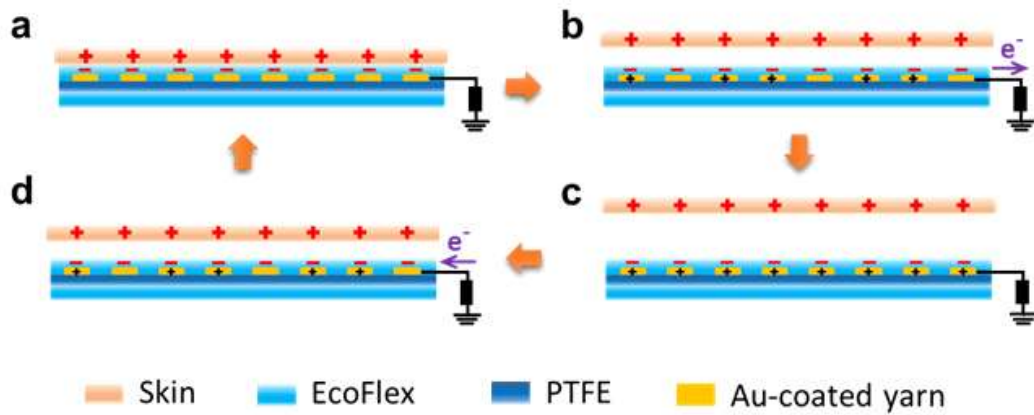


Figure 3.2. (a-d) Electricity generation mechanism of on-body-based soft TENG.

3.2.2. Output performance

Figure 3.3 displays the evaluation of the mechanical and electrical properties of the on-body-based soft TENG. The tensile strength was determined using a tensile tester, as shown in figure 3.3(a), to evaluate the mechanical properties. The tensile strength can be measured through the load and the stretching degree until the sample is cut when pulled in the axial direction of the sample. The deformation rate was increased at a constant speed, and the required load was measured to obtain the load-deformation curve (figure 3.3(b)). A maximum load of 3.3 N occurred, and the material broke at 560% strain. As the electrode Au-coated yarns were formed in a serpentine shape, they were not damaged even at high strain rates, and the yarns had a minimal effect on the stiffness of TENG.

A $7 \times 4 \text{ cm}^2$ TENG was evaluated to determine the electrical output performance. The on-body-based soft TENG generated energy during a stretching motion owing to its flexibility and elasticity, as well as contact separation movements with the skin. A digital oscilloscope with an internal impedance of $1 \text{ M}\Omega$ and a precision source/measurement device generated an open circuit voltage of 280 V and a module short circuit current of $12 \text{ }\mu\text{A}$ at approximately 1 kgf of contact separation motion (figures 3.4(a) and (b)). Similarly, a 140 V and a $3 \text{ }\mu\text{A}$ were generated through the stretching motion in the same environment (figures 3.4(c) and (d)). The output power was measured at a load of $1 \text{ k}\Omega$ - $100 \text{ M}\Omega$ to evaluate the output performance in detail. Figure 3.4(e) shows the measured voltage and current based on the resistance change attributed to the stretching motion. As the load resistance increased, the output voltage also increased and became saturated after $100 \text{ M}\Omega$. In contrast, the output current decreased when the load resistance increased. The maximum output power density was calculated using $W = V_{\text{peak}}^2/R$, as shown in figure 3.4(f), and reached 150 mW/m^2 at a load resistance of $10 \text{ M}\Omega$.

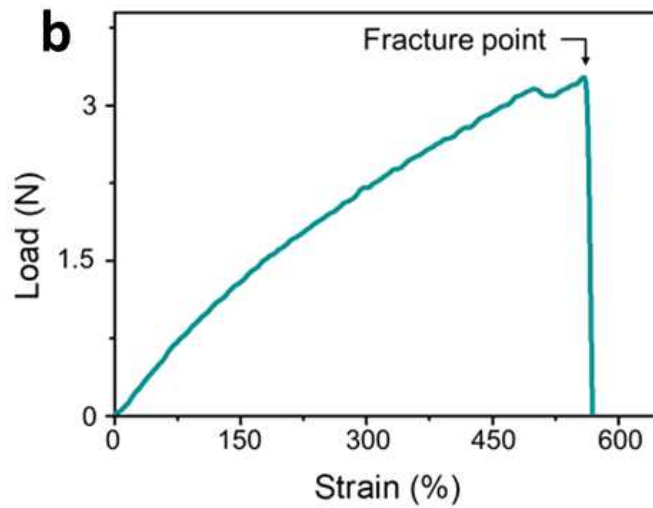
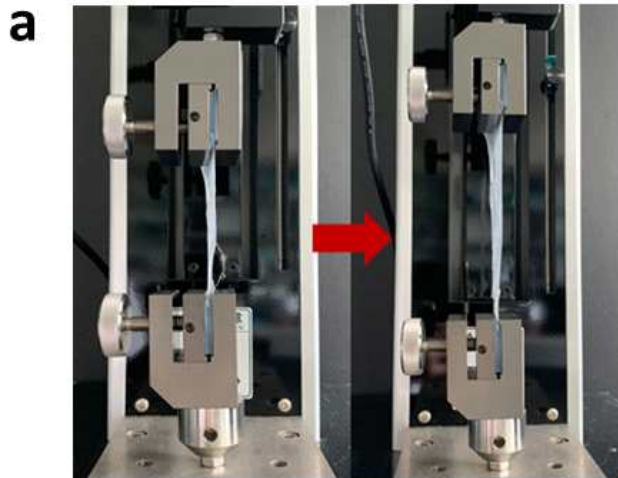


Figure 3.3. (a) Photograph of the experimental setup for the tensile strength test. (b) Load deformation curve.

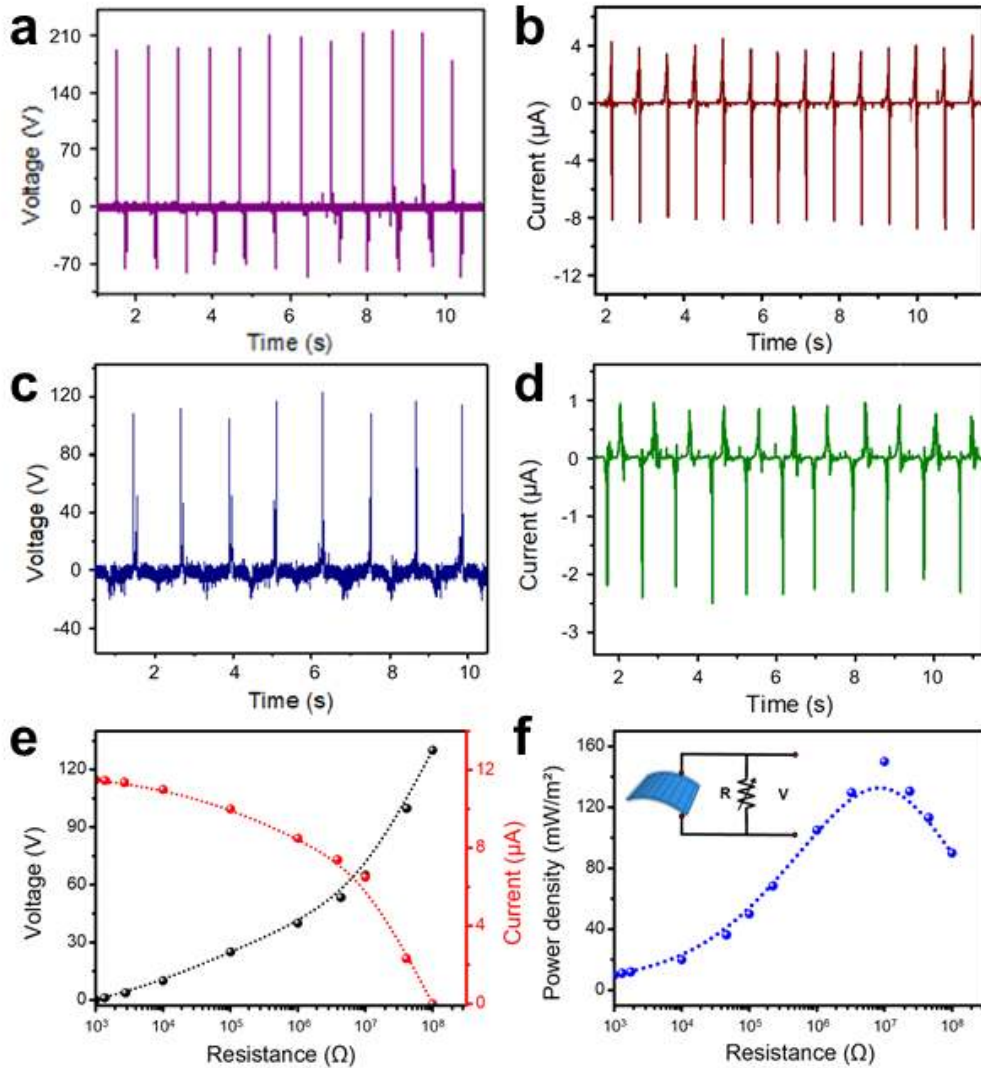


Figure 3.4. (a, b) Electrical outputs under contact separation motion and (c, d) stretching motion. (e) Dependence of the output voltage and current on the external load resistance. (f) Output power per square meter of the on-body-based soft TENG.

3.2.3. Stability and durability

In addition, good mechanical stability and durability are vital factors that are required to meet the reliability demands for TENGs. As shown in figure 3.5(a), a constant force (0.5 kgf) was applied to the TENG using a pushing tester for testing under the cyclic compression force. As shown in figures 3.5(b) and (c), a stable signal was generated without distorting the output voltage and current under 2,500 pushing cycles. These results demonstrated the practical robustness and mechanical durability of the developed TENG.

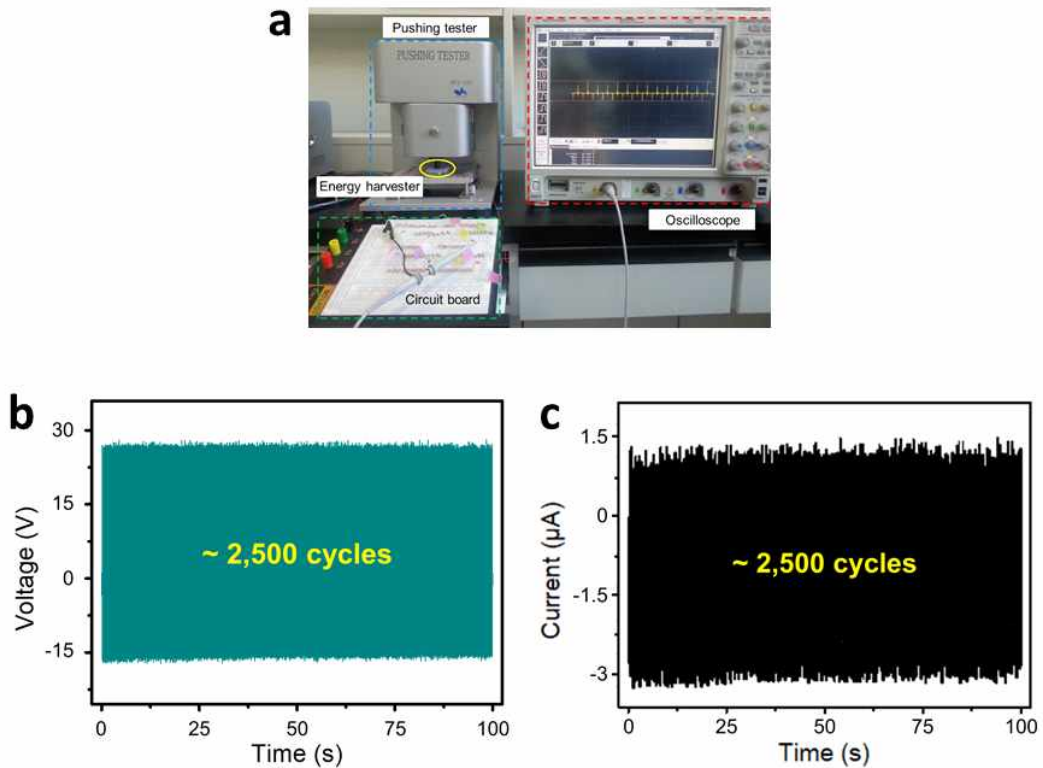


Figure 3.5. (a) Photograph of experimental setup for pushing test. (b) Output voltage and (c) current from durability test under 2500 cycles.

An initial state of 70% strain and output were measured after a cycle using a tensile tester, as shown in figure 3.6(a), to maintain the flexibility. As shown in figures 3.6(b) and (c), it was confirmed that no degradation in performance occurred even after prolonged use by outputting a constant voltage and current signal after repeated deformations for 2,500 cycles. Based on the flexible characteristics of on-body-based soft TENGs, the energy generation in various motions, and the excellent durability, TENGs have a practical application as reliable energy-harvesting devices.

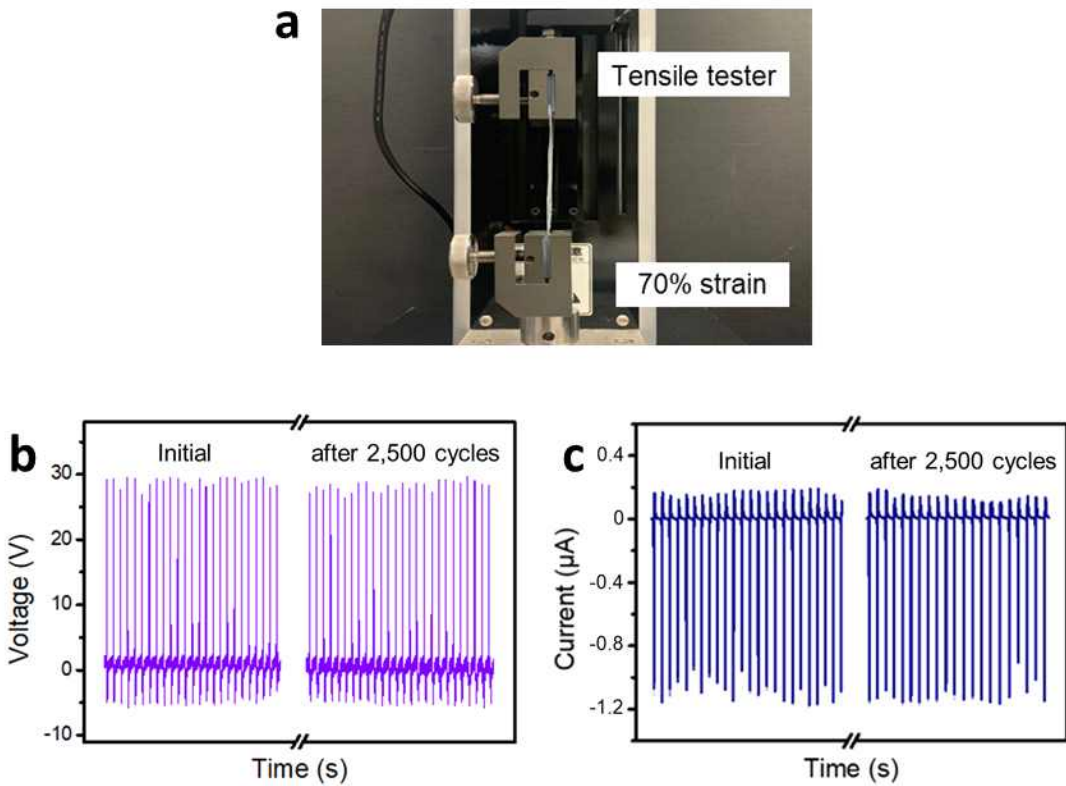


Figure 3.6. (a) Photograph of experimental setup for tensile test. (b) Output voltage and (c) current before and after stretching under 2500 cycles.

3.2.4. Practical applications

The power generated from the TENG can be stored in elements, such as capacitors or condensers, to drive electronic devices, which demonstrate the practical application of the on-body-based soft TENG. As shown in figure 3.7(a), a circuit was constructed by connecting a 2.2 μF capacitor to the self-storage device to drive the electronic clock. The circuit included a bridge circuit for converting alternating current to direct current (DC). The TENG continuously drove the electronic watch through contact-separation movement when attached to the back of the hand (figure 3.7(b)). Moreover, the on-body-based soft TENG could be used to charge the capacitor for lighting the LED. With a DC supply, an LED requires a minimum driving voltage of 1.8 V. As depicted in figure 3.7(c), an external force was applied to the TENG attached to the back of the hand to charge a 1 μF capacitor and to supply power to the LED. The six LEDs were connected in series, which required a driving voltage of 10.8 V, such that the voltage charged in the capacitor adequately lighted up the device (figure 3.7(d)). A 1 μF capacitor can be charged to 12 V in approximately 30 s. According to the formula $Q = CV$, the amount of charge stored in a 1 μF capacitor charged for more than 30 s is approximately 30 μC . Therefore, TENG has the potential of being used as a self-powered body-attached power source, as it generates energy, charges capacitors adequately, and drives electronics. The soft TENG developed in this study was attached to various parts of the human body to verify that biomechanical energy could be harvested during human body movements. The soft TENG generated stable output voltage and current through the application of contact-separation and stretching-release force based on human motion. Owing to its excellent deformability, TENG wholly adhered to the skin, even during the motion of the human body. As shown in figures 3.7(e) and (f), the soft TENG attached to the human wrist generated 30 V and 0.95 μA during the flexion and extension of the wrist. Next, it was attached to the inside of

the elbow, where it generated 40 V and 1.4 μA during the folding and unfolding of the arm. To exploit the walking energy, the soft TENG was worn under the foot, where it generated 42 V and 1.5 μA during the stepping motion. The on-body-based soft TENG is flexible, stretchable, easy to manufacture, and suitable for the human body. As various E-skin and Internet-of-things systems that can be driven with low power have been developed, soft TENGs are expected to be used as next-generation self-supporting energy power sources that can be utilized semi-permanently without batteries.

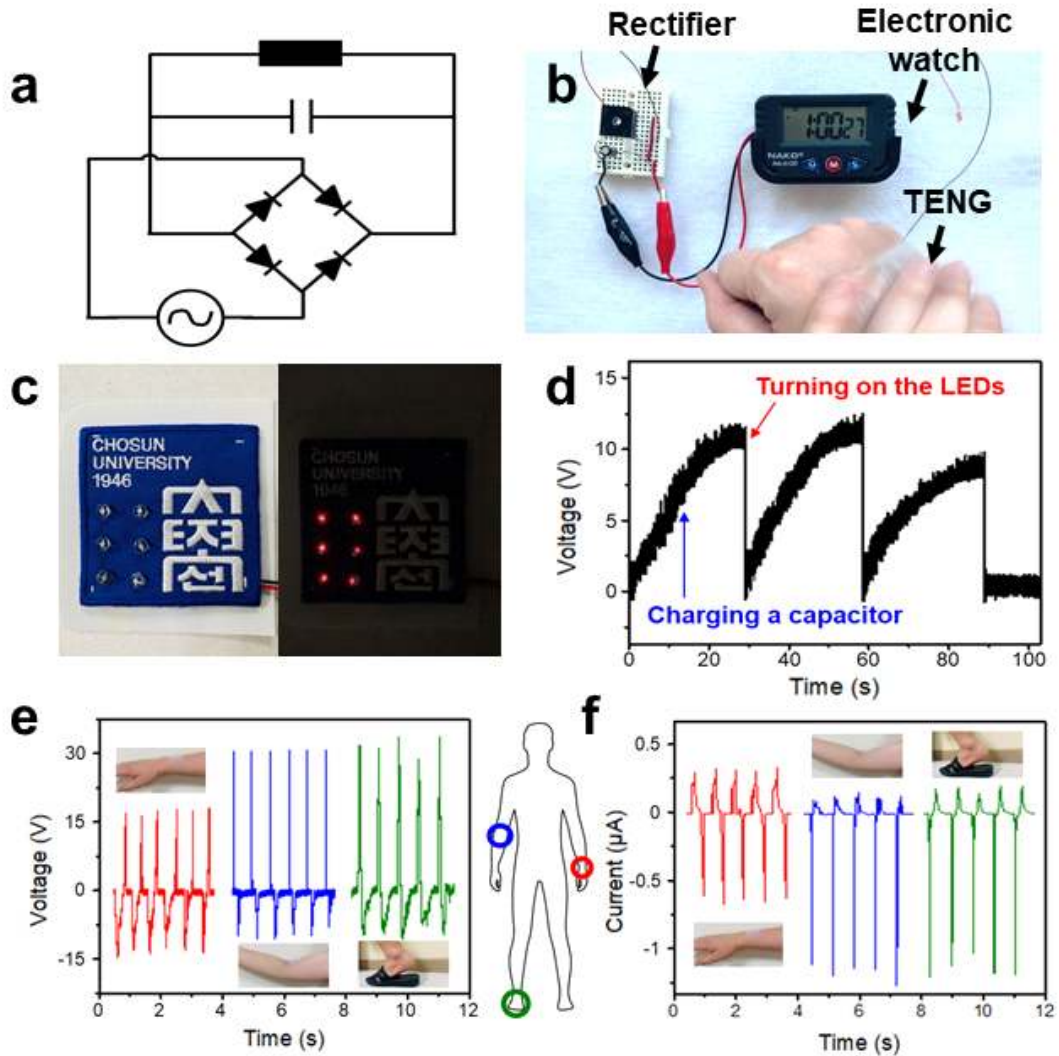


Figure 3.7. (a) Circuit diagram of a full-wave bridge rectifier. (b) Electronic watch powered using a soft TENG. (c) Commercial LEDs directly lighted and visible in a dark environment. (d) Charging capability of on-skin-based soft TENG on a commercial capacitor of 1 μF . (e) Output voltages and (f) current of soft TENG mounted on different body parts.

IV. TENG-based E-skin

4.1. Experimental details

4.1.1. Fabrication of the patterned PDMS films

In this study, PDMS was selected as the substrate and an insulating material. The micro/nano pattern on the surface of the PDMS film leads to increases the sensitivity and response time compared to those of a flat PDMS film [61]. Polytetrafluoroethylene (PTFE)-coated glass fabric tape with a knitting pattern was used for fine patterning on the PDMS film. The PTFE-coated glass fabric tape shows the texture of a microscale surface. The PDMS elastomer and curing agent were stirred in a 10:1 ratio. As shown in figure 4.1(a), the mixture was coated on a glass sheet with PTFE tape attached. A desiccator was used to remove air bubbles from the PDMS mixture. The glass sheet was fixed by floating it vertically in the air. The solution was then cured, allowing it to fall downwards. It was heated to 75 °C for 2 hours in an oven and cured at room temperature for more than 24 hours. Then, when the PDMS film was peeled off from the glass sheet, a reverse pattern for the PTFE tape surface was molded onto the film surface. The surface of the PTFE tape was easily peeled off the PDMS film owing to its nonstick property. The thickness of the PDMS film was in the range of $200 \pm 15 \mu\text{m}$. A field emission scanning electron microscope (FESEM) image of the surface of the PTFE tape and the patterned PDMS film is shown in figure 4.1(b) and (c).

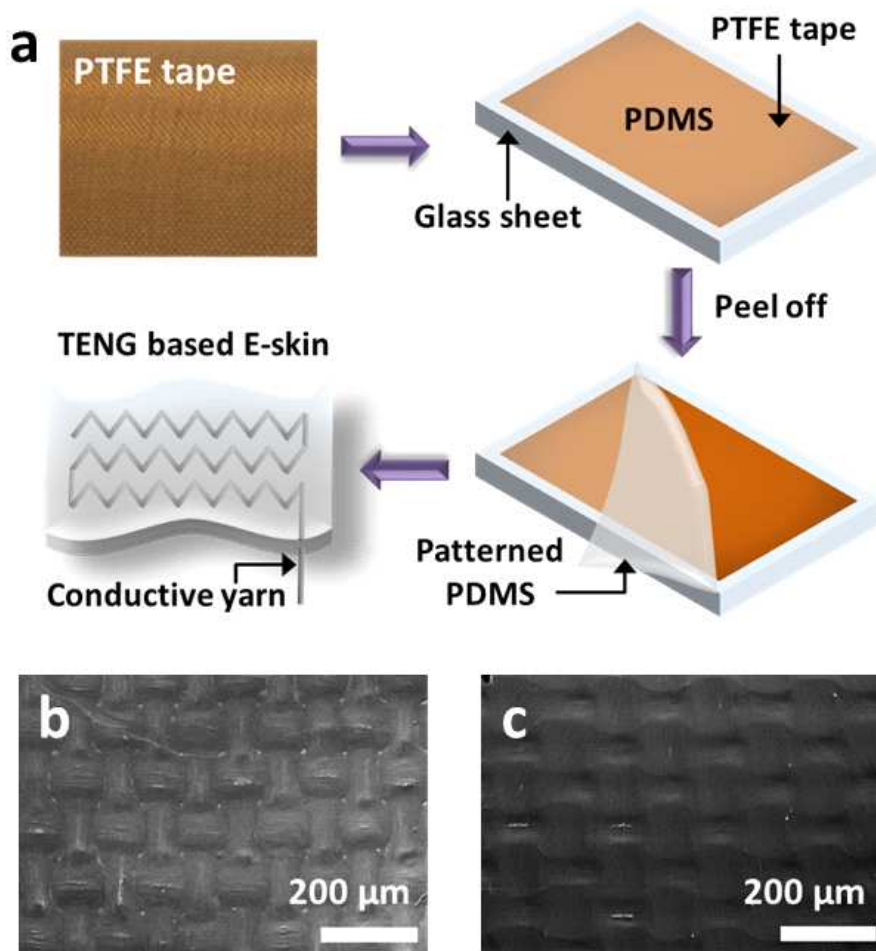


Figure 4.1. (a) Schematic of the fabrication process of patterned PDMS films and TENG-based E-skin. (b) FESEM images of PTFE-coated glass fabric tape and (c) patterned PDMS film, respectively.

4.1.2. Fabrication of electrode layer and TENG-based E-skin

The electrode located between the two PDMS films utilizes conductive yarn and is formed in a zigzag pattern. The ESLAST ES-5772 silicone sealant can be used to fix the zigzag-patterned conductive yarns to PDMS films. This sealant was cured at room temperature for 5 min. The conductive yarn was selected as the electrode material because of its excellent electrical conductivity, easy accessibility, and low resistance. Conductive yarn is a structure in which three strands of Ag-coated Cu yarn and polyester are twisted together and have a thickness of 199 μm and a conductivity of 0.049 Ω/cm (figure 4.2(a)). The FESEM image of the side of the conductive yarn is shown in figure 4.2(b). Figure 4.2(c) is an 80 times magnified field emission transmission electron microscope (FETEM) image of the vertical section of the TENG-based E-skin. The grids in the image are nickel TEM grids, and the image shows the overall cross-sectional of the conductive yarn electrode. Figure 4.2(d) is Ag-coated Cu yarn of the conductive yarn and figure 4.2(e) is a part of the polyesters. Figure 4.2(f) shows the fabricated TENG-based E-skin (area of $50 \times 40 \text{ mm}^2$). The zigzag pattern using conductive yarn is uniformly formed on the PDMS film, and if the E-skin TENG is stretched in the transverse direction, the yarn is stretched in the same direction. Therefore, it can be deformed according to the movement of the body and can easily attach to curved body parts.

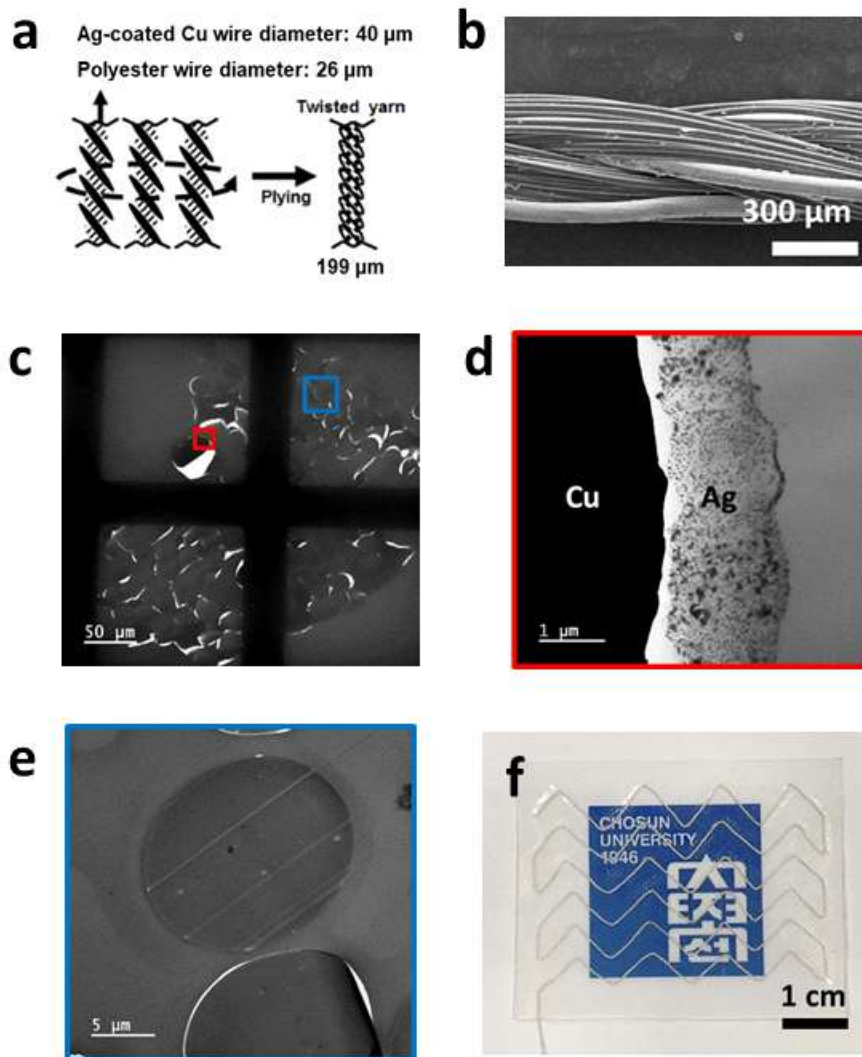


Figure 4.2. (a) Schematic of the structure of the conductive yarn. (b) FESEM image of the side of the conductive yarn. (c) FETEM images of the longitudinal section of TENG-based E-skin and conductive yarn electrode including (d) Ag-coated yarn and (e) polyesters. (f) Photograph of TENG-based E-skin.

4.1.3. Characterization and measurement

The PTFE tape, patterned PDMS film, and conductive yarn were used to study the morphology using a Hitachi S-4800 field emission scanning electron microscope and a JEM-2100F field emission transmission electron microscope. The open-circuit voltage was measured using an MSO9104A digital oscilloscope, whereas the short-circuit current was measured using a B2911A precision source/measurement device. The applied force was measured using a CI-10W digital indicator. A JIPT-100 pushing tester was employed to drive the TENGs under cyclic compression force and to test its stability. An MCT-2150 tensile tester was used to measure the elasticity. Electrical output performance of body-attachable TENG-based E-skin was directly measured using practical hand tapping.

4.2. Results and discussion

4.2.1. Working mechanism

As shown in figure 4.3, the TENG-based E-skin operates in the single-electrode mode by connecting the conductive yarn to the ground without an additional metal wire. PDMS is a negatively charged material that forms a triboelectric layer, whereas the skin is positively charged and is considered an electrostatic layer. When the skin is in contact with the PDMS film of TENG-based E-skin, a triboelectric charge occurs at the interface of the two materials and generates the same amount of charge with opposite polarities on each surface (figure 4.3(i)). When the skin separates and moves away from the PDMS film, a potential difference is generated between the two materials. The generated potential difference can bias the external circuit to the ground and output the current (figure 4.3(ii)). When the skin and PDMS film are maximally separated, an electrostatic equilibrium is formed (figure 4.3(iii)). When the skin approaches the PDMS film, the entire process is reversed, and the current flows in the opposite direction (figure 4.3(iv)). Thus, the contact-separation process of the two materials by an external force creates a continuous alternating current (AC). The generated AC output current is shown in the inset. When the skin was in contact with the PDMS film, the open-circuit voltage (V_{oc}) and short-circuit charge quantity (Q_{sc}) were all zero. Conversely, when the two materials are far apart, V_{oc} and Q_{sc} can be derived as [62]

$$\begin{aligned}
 V_{oc} &= -\sigma A/2C_0 \\
 Q_{sc} &= -\sigma A/2
 \end{aligned}$$

where σ is the density of the electrostatic charge generated on the surface of the PDMS film, C_0 the capacitance of the TENG-based E-skin, and A the contact area between the skin and PDMS.

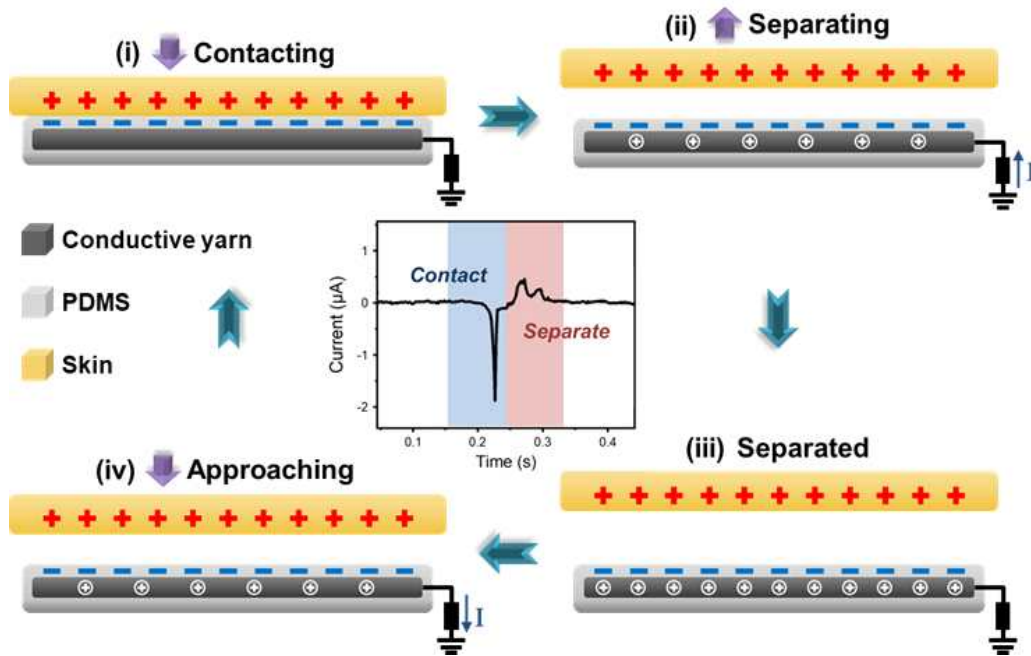


Figure 4.3. Schematic of the principle of the TENG-based E-skin in single-electrode mode. Current output under one cycle of contact and separation is shown in the figure.

4.2.2. Output performance and stability

A tensile-strength test was performed to evaluate the mechanical properties of the TENG-based E-skin. As shown in figure 4.4, the device experienced a stress of 143 kPa at a stretch ratio of 4.8. The inset of figure 4.4 shows the relationship between the stretching strain and resistance of the conductive yarn. The conductivity of the conductive yarn is almost independent of the stretch ratio by applying the change in resistance $R/R_0 = \lambda^2$ to the stretch ratio λ . In other words, it is possible to ensure both the stable conductivity of the conductive yarn and performance of the device under tensile strain.

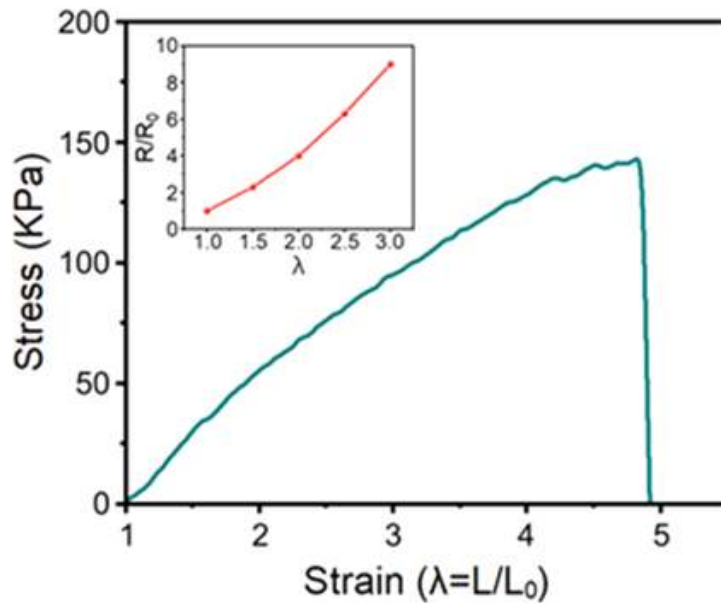


Figure 4.4. Stress-strain of the TENG-based E-skin. Inset is the resistance change of the conductive yarn with stretching strains.

The energy harvesting performance of the TENG-based E-skin was evaluated by applying a cycling contact-separation motion. In general, the open-circuit voltage (V_{oc}) and short-circuit current (I_{sc}) are important parameters for analyzing the performance of a TENG. TENG-based E-skin (area of $70 \times 50 \text{ mm}^2$) generates an output of approximately 200 V (figure 4.5(a)) and $2.7 \mu\text{A}$ (figure 4.5(c)) at a pressure of approximately 1 kgf during periodic contact-separation of the skin. The response and recovery time are important parameters for evaluating the sensor performance of TENG-based E-skins. As shown in figure 4.5(b), the response and recovery times of the device were 18 and 89 ms, respectively. This shows a faster response to biomechanical energy collection and external pressure than other reported TENGs [63, 64]. The actual power density depends on the device load. A load of $10 \text{ K}\Omega$ - $10 \text{ G}\Omega$ was connected to the electrode of the TENG-based E-skin, and the electrical output was measured. As shown in figure 4.5(d), the output voltage increases and saturates as the external load increases, whereas the output current decreases according to Ohm's law. The output power density was calculated as $P = I^2R$ [65]. As shown in figure 4.5(e), the output power density at an external load of $100 \text{ M}\Omega$ reached the maximum value, that is, 154 mW/m^2 .

In addition, to investigate the stability and durability, the voltage and current of the TENG were measured during contact-separation with a force of 0.2 kgf for 4,500 cycles. As shown in figure 4.6(a) and (b), no significant reductions in V_{os} or I_{sc} were observed after repeated cycles. This excellent mechanical stability demonstrates the robustness and practical value of the device and meets the reliability requirements. Stability and durability tests were conducted using a pushing tester, as shown in figure 4.6(c). A contact force of 3 cycles per second can be applied to a TENG with an area of 113.04 mm^2 . In addition, the TENG-based E-skin could be stretched by up to 30% (figure 4.6(d)). Because the skin of the human arm can withstand a maximum deformation of up to 27% [66], the device can operate properly

under general physical conditions when attached to the skin.

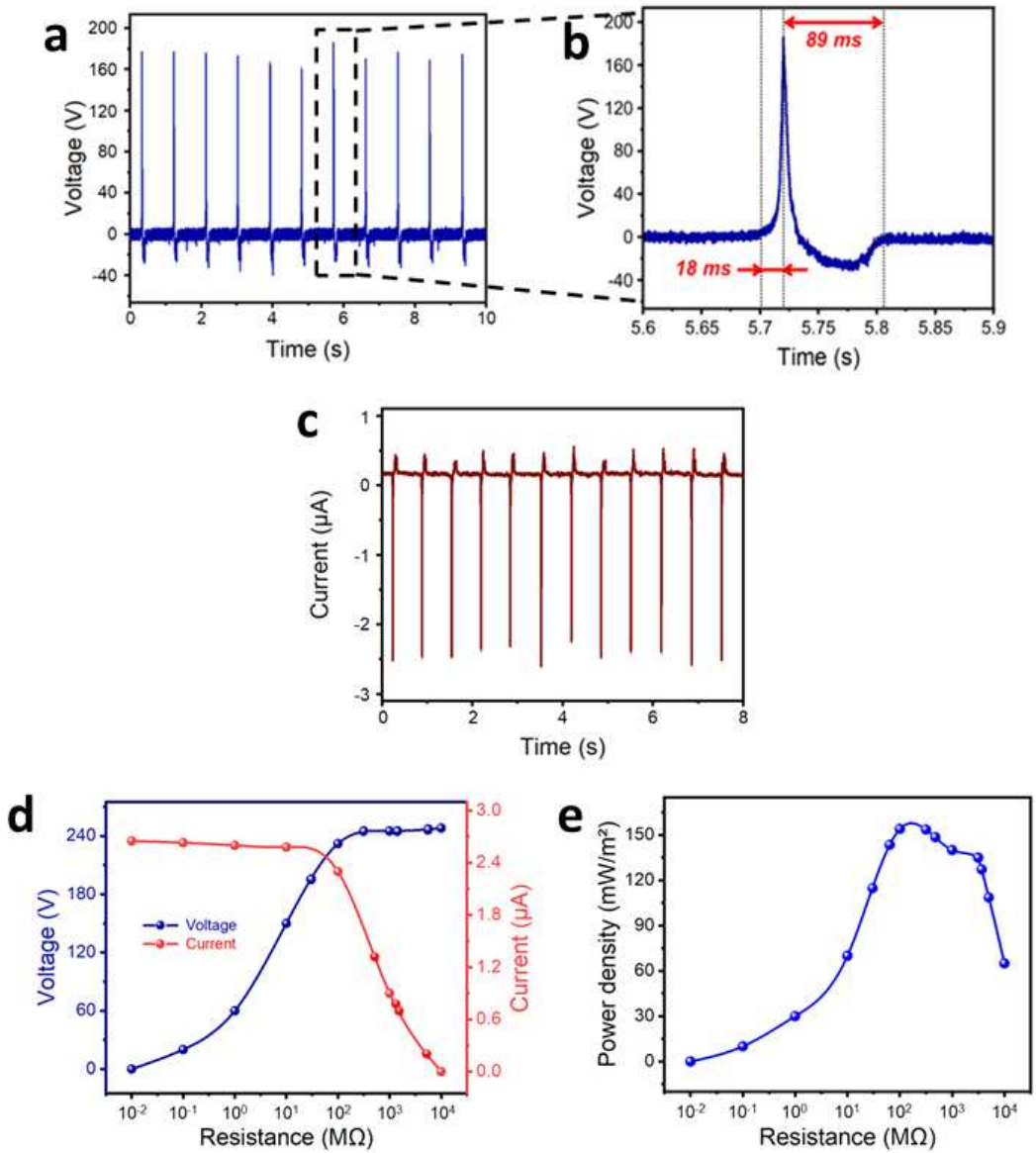


Figure 4.5. Electrical output performance including (a) V_{oc} , (b) response and recovery time of V_{oc} by the dashed black box, and (c) I_{sc} . (d) The measured voltage, current, and (e) power density of the external load resistances.

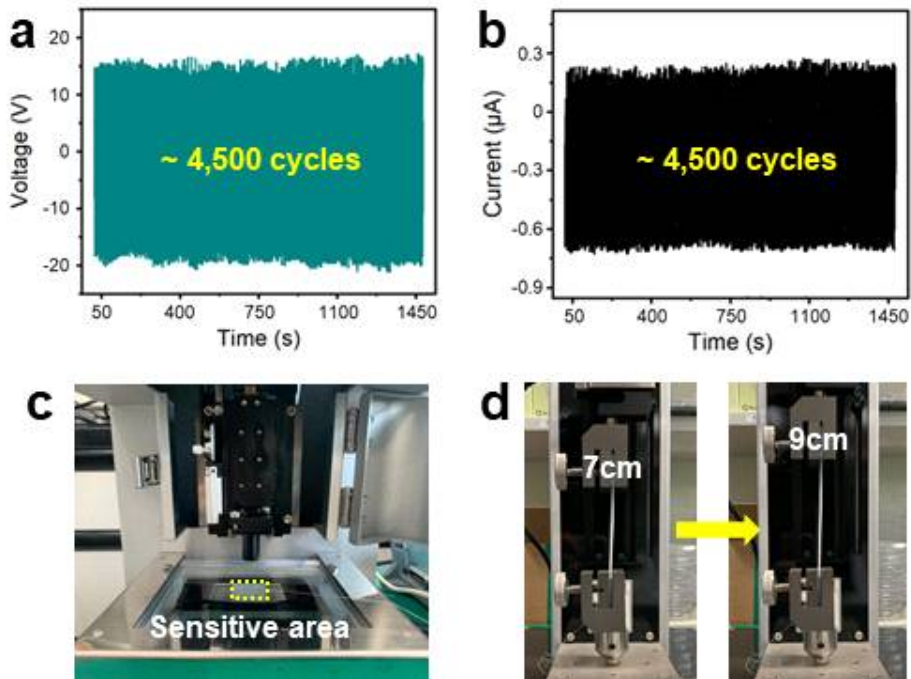


Figure 4.6 (a) V_{oc} and (b) I_{sc} from durability test under ~ 4500 cycles of contact-separation motions. (c) Photographs of the cycling test setup with a pushing tester and (d) TENG-based E-skin at the initial state and 30% strain.

4.2.3. Comparison of the transparent and flexible TENGs

The excellent electrical properties of this TENG showed better performance than those found in recently reported research. As shown in table 4.1, the TENG-based E-skin exhibited an outstanding electrical output performance compared to [50, 67, 68], respectively; it showed good stability compared to [67, 68, 69]; further, it showed a fast response time compared to [70], and has a thin total thickness compared to [70, 71]. As in [71], when the thickness of the TENG is thick, the stability and output performance are good, but it is difficult to attach to human skin. In the future, optimizing the thickness of TENG-based E-skin is expected to improve the fit and reach a response time of < 10 ms. Moreover, as the PDMS film becomes thinner, the capacitance between the skin surface and the conductive yarn electrodes will increase, which will improve the output performance. The excellent properties of TENG-based E-skin are best suited for biomechanical energy harvesting and multi-purpose self-wearable sensors.

| Materials | Electrical output | Stable cycles | Response time | Total thickness | Ref. |
|--|-----------------------|---------------|----------------------------|-----------------|-----------|
| Elastomer tape and Carbon grease | 115 V and 3 μ A | 2,000 | Only detects body movement | 102 μ m | [69] |
| PDMS, AgNW, and silk solution | 2 mW/m ² | 2,500 | 7 ms | 120 μ m | [67] |
| Elastomer (PDMS or VHB) and Hydrogel | 35 mW/m ² | 5,000 | Only detects body movement | 260 μ m | [50] |
| Si-rubber and Silver-coated nylon yarn | 240 mW/m ² | 50,000 | Only detects body movement | 2,800 μ m | [71] |
| PDMS, PVDF, and AgNWs | 57 mW/m ² | 1,000 | 65 ms | 660 μ m | [70] |
| EcoFlex and PTFE | 150 mW/m ² | 2,500 | Only detects body movement | 400 μ m | [68] |
| PDMS and Ag-coated Cu yarn | 154 mW/m ² | 4,500 | 18 ms | 400 μ m | This work |

Table 4.1. Comparison of energy harvesting and self-powered sensing characteristics of various transparent and flexible TENGs.

4.2.4. Practical applications

The electrical output of TENG-based E-skin can be used to continuously power portable electronic products. The equivalent circuit for storage in an energy storage device or used as a power source for the device is shown in figure 4.7(a). The skin and TENG-based E-skin were connected to the bridge circuit. Figure 4.7(b) shows that the AC generated from the TENG-based E-skin was rectified to direct current (DC) by the bridge circuit. A 1 μF capacitor was charged at a frequency of 5 Hz to determine whether it could actually be applied to the device. The capacitor voltage increased to 5 V for approximately 45 s, and thus the quantity of electric charge was approximately 5 μC (figure 4.7(c)). An electronic watch can be operated by attaching a TENG to the left hand and tapping with the right hand (figure 4.7(d)). In addition to the self-storage element built into the electronic watch, it charged a 2.2- μF capacitor and supplied power through a bridge circuit. For an application experiment with a large strain, a TENG-based E-skin (area of $60 \times 25 \text{ mm}^2$) was attached to the wrist, and the output signal depending on the bending of the wrist was measured. The device was stretched by up to 18% by bending the wrist. As shown in figure 4.7(e), the result of comparing the output before and after deformation by hand tapping showed stable triboelectric performance. This demonstrates the excellent flexibility of the device and its ability to harvest energy by attaching it to various parts of the body. TENG-based E-skin can detect subtle physiological signals, such as wrist arterial pulses, owing to its high sensitivity. To measure the pulse without moisture on the skin, the attached area of the wrist was wiped with alcohol gauze. A TENG (area of $20 \times 20 \text{ mm}^2$) was attached to the wrist, and the arterial pulse was monitored, as shown in figure 4.7(f). Therefore, these experimental observations indicate that the wearable systems can potentially utilize TENG-based E-skin to harvest energy, power electronics, and monitor human signals.

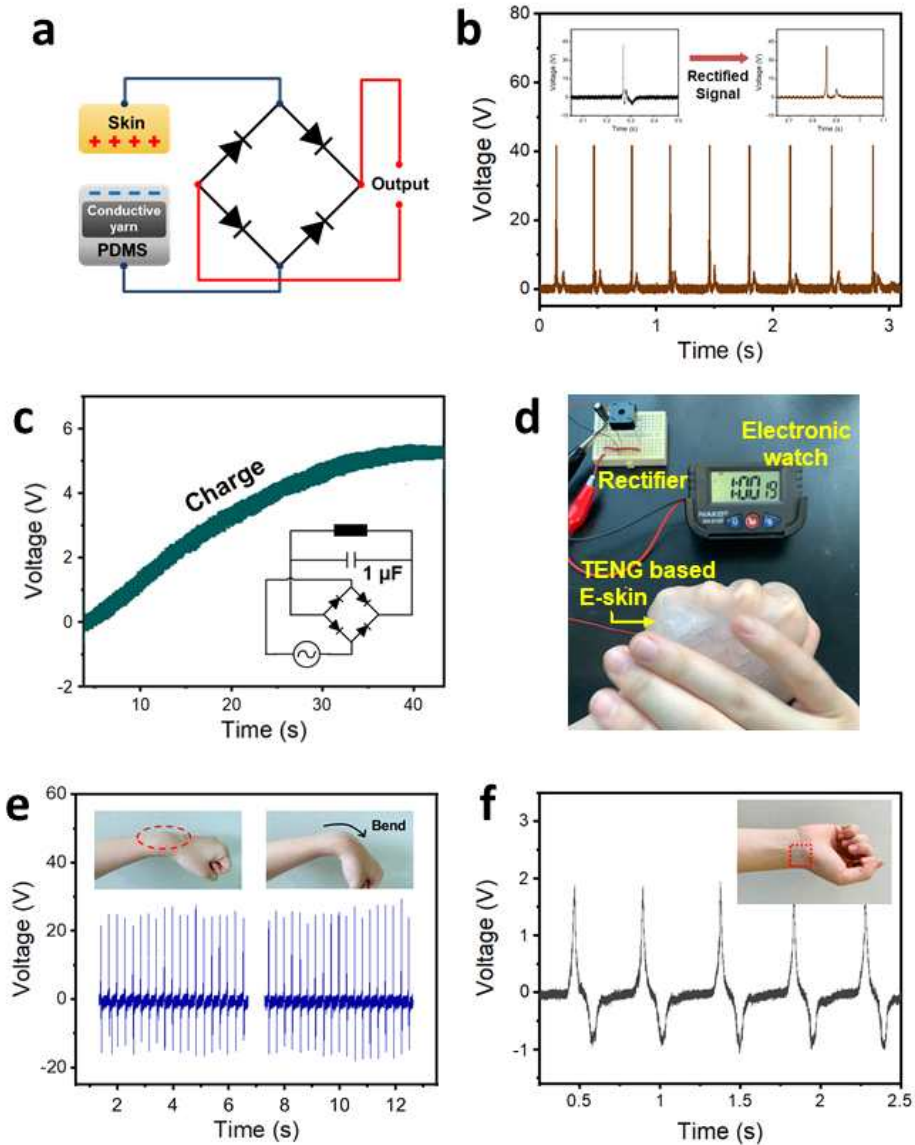


Figure 4.7. (a) Schematic of the equivalent circuit of a full-wave bridge rectifier. (b) Rectified voltage signal of a pulse signal input. (c) Capacitor charging at a frequency of 5 Hz. (d) Demonstration of powering an electronic watch by hand tapping the TENG-based E-skin. (e) Electrical output before and after bending the wrist. (f) Real-time arterial pulse waves. Inset is a photograph of a TENG-based E-skin on a wrist.

V. Conclusion

In this study, a fiber-type, woven-structured, body-attached, and E-skin-type TENG was developed. The developed TENG harvests the energy generated by body movements and can thus be applied to wearable electronics. Elasticity and durability were secured by compounding the polymer elastomer and conductive yarn. The power generation performance of the E-skin type TENG was improved by micro/nano patterning the surface of the triboelectric material using an efficient casting method. It was also applied as an integrated pressure sensor to detect biosignals. Consequently, the core requirements of TENG were met, and the influence of parameters, such as the physical and micro/nano-scale electrical characteristics of TENG, according to each type was analyzed.

First, a highly stretchable FTENG and flexible WTENG were fabricated using silicone rubber and conductive thread. The WTENG consists of a single-strand of a long FTENG. As a single-electrode structure harvesting the mechanical energy generated from free motions, the proposed WTENG generated $34.4 \mu\text{W}/\text{cm}^2$ power from continuous contact with the skin. The WTENG demonstrated outstanding durability without degrading the electrical output during the application of repetitive external forces at 5000 pushing cycles. It was demonstrated to power a commercial LED and electrical watch with the output energy, as examples for practical applications. In addition, its potential for converting the mechanical energy generated from human motion into electric energy was illustrated. The theoretical and experimental results establish that the WTENG can be utilized as a self-powered system and can offer a new solution to power wearable or portable devices.

Second, a highly stretchable on-body-based soft TENG was developed for use as an energy-generating skin using an EcoFlex elastomer and Au-coated

yarns. The electrodes were formed in a serpentine shape, which allowed energy to be generated durably without damaging the device, even under high deformation. Its ultra-thin thickness (200 μm) and high elasticity (>100%) made it easily attachable to the skin or body curves, allowing for unrestricted body motions. An on-body-based soft TENG was attached to the back of the hand to produce 150 mW/m^2 power through continuous skin contact and remained stable without signal degradation during repeated cycles of 2500 external forces. The TENG has a practical application potential because it can charge a capacitor and drive an electronic watch and LEDs, and can also be used to harvest mechanical energy generated from human motion. This may function as a new soft battery capable of supplying power to an electronic skin or a wearable device. Therefore, the development of stretchable and flexible TENGs is expected to be used in artificial muscles, wearable sensors, human-machine interfaces, and power supply for various devices in the future.

Last, we developed a soft and transparent TENG-based E-skin as a type of energy harvesting and pressure sensor by combining a uniform micro-patterned PDMS film and conductive yarn. The inverted micro-pattern was replicated on the surface of the PDMS film using a fine knitted pattern of PTFE tape as a mold. The conductive yarn is composed of an Ag-coated Cu yarn and a polyester, which forms an electrode layer in a zigzag pattern to impart elasticity, stability, and high sensitivity of the TENG. As an energy harvesting device, it can generate a power of 154 mW/m^2 and can charge a capacitor and power an electronic watch. It has also demonstrated a fast response time and outstanding stability over 4500 pushing cycles. With a self-pressure sensor, it detects the wrist arterial pulse and shows the capability to monitor human physiological signals in real-time. This hybrid TENG-based E-skin is expected to be applicable to applications such as wearable power supplies, biological monitoring, and self-powered motion detection sensors owing to its advantages such as simple manufacturing and low cost.

Reference

- [1] H. Wang, A. Jasim and X. Chen, “Energy harvesting technologies in roadway and bridge for different applications - A comprehensive review”, *Applied Energy*, vol. 212, 1083-1094, Feb. 2018.
- [2] H. Ryu, H.-J. Yoon and S.-W. Kim, “Hybrid energy harvesting: Toward sustainable energy harvesting”, *Advanced Materials*, vol. 31, 1802898, Feb. 2019.
- [3] Z. L. Wang, J. Chen and L. Lin, “Progress in triboelectric nanogenerators as a new energy technology and self-powered sensors”, *Energy&Environmental Science*, vol. 8, 2250-2282, Jun. 2015.
- [4] H.-J. Yoon, H. Ryu and S.-W. Kim, “Sustainable powering triboelectric nanogenerators: Approaches and the path towards efficient use”, *Nano Energy*, vol. 51, 270-285, Sep. 2018.
- [5] L. Xie and M. Cai, “Human motion: Sustainable power for wearable electronics”, *IEEE Pervasive Computing*, vol. 13, 42-49, Oct.-Dec. 2014.
- [6] R. Kakihara, K. Kariya, Y. Matsushita, T. Yoshimura and N. Fujimara, “Investigation of piezoelectric energy harvesting from human walking”, *Journal of Physics: Conference Series*, vol. 1052, 012113, Nov. 2017.
- [7] C. Dagdeviren, B. D. Yang, Y. Su, P. L. Tran, P. Joe, E. Anderson, J. Xia, V. Doraiswamy, B. Dehdashti, X. Feng, B. Lu, R. Poston, Z. Khalpey, R. Ghaffari, Y. Huang, M. J. Slepian and J. A. Rogers, “Conformal piezoelectric energy harvesting and storage from motions of the heart, lung, and diaphragm”, *PNAS*, vol. 111, 1927-1932, Feb. 2014.

- [8] C. Dagdeviren, S.-W. Hwang, Y. Su, S. Kim, H. Cheng, O. Gur, R. Haney, F. G. Omenetto, Y. Huang and J. A. Rogers, “Transient, biocompatible electronics and energy harvesters based on ZnO”, *Small*, vol. 9, 3398-3404, Apr. 2013.
- [9] V. Leonov and R. J. M. Vullers, “Wearable thermoelectric generators for body-powered devices”, *Journal of Electronic Materials*, vol. 38, 1491-1498, Jan. 2009.
- [10] Y. K. Ramadass and A. P. Chandrakasan, “A battery-less thermoelectric energy harvesting interface circuit with 35 mV startup voltage”, *IEEE Journal of Solid-State Circuits*, vol. 46, 333-341, Jan. 2011.
- [11] Z. Lin, J. Chen, X. Li, Z. Zhou, K. Meng, W. Wei, J. Yang and Z. L. Wang, “Triboelectric nanogenerator enabled body sensor network for self-powered human heart-rate monitoring”, *ACS Nano*, vol. 11, 8830-8837, Aug. 2017.
- [12] Z. L. Wang, “Triboelectric Nanogenerators as new energy technology for self-powered systems and as active mechanical and chemical sensors”, *ACS Nano*, vol. 11, 9533-9557, Sep. 2013.
- [13] J. Park, A. Y. Choi, C. J. Lee, D. Kim and Y. T. Kim, “Highly stretchable fiber-based single-electrode triboelectric nanogenerator for wearable devices”, *RSC Advanced*, vol. 7, 54829-54834, Dec. 2017.
- [14] M.-G. Kang, W.-S. Jung, C.-Y. Kang and S.-J. Yoon, “Recent progress on PZT based piezoelectric energy harvesting technologies”, *Actuators*, vol. 5, 5, Feb. 2016.
- [15] F. Narita and M. Fox, “A review on piezoelectric, magnetostrictive, and magnetoelectric materials and device technologies for energy harvesting applications”, *Advanced Engineering Materials*, vol. 20, 1700743, Nov. 2017.

- [16] H. Jouhara, A. Z.-Gora, N. Khordehgah, Q. Doraghi, L. Ahmad, L. Norman, B. Axcell, L. Wrobel and S. Dai, “Thermoelectric generator (TEG) technologies and applications”, *International Journal of Thermofluids*, vol. 9, 100063, Feb. 2021.
- [17] S. Karabetoglu, A. Sisman, Z. F. Ozturk and T. Sahin, “Characterization of a thermoelectric generator at low temperatures”, *Energy Conversion and Management*, vol. 62, 47–50, Oct. 2012.
- [18] J. Park, D. Kim, A. Y. Choi and Y. T. Kim, “Flexible single-strand fiber-based woven-structured triboelectric nanogenerator for self-powered electronics”, *APL Materials*, vol. 6, 101106, Oct. 2018.
- [19] C. Wu, A. C. Wang, W. Ding, H. Guo and Z. L. Wang, “Triboelectric nanogenerator: A foundation of the energy for the new era”, *Advanced Energy Materials*, vol. 9, 1802906, Nov. 2018.
- [20] P. Bai, G. Zhu, Z.-H. Lin, Q. Jing, J. Chen, G. Zhang, J. Ma and Z. L. Wang, “Integrated multilayered triboelectric nanogenerator for harvesting biomechanical energy from human motions”, *ACS Nano*, vol. 7, 3713–3719, Mar. 2013.
- [21] J. Park, D. Kim and Y. T. Kim, “Soft and transparent triboelectric nanogenerator based E-skin for wearable energy harvesting and pressure sensing”, *Nanotechnology*, vol. 32, 385403, Jul. 2021.
- [22] S. Khalid, I. Raouf, A. Khan, N. Kim and H. S. Kim, “A review of human-powered energy harvesting for smart electronics: Recent progress and challenges”, *International Journal of Precision Engineering and Manufacturing-Green Technology*, vol. 6, 821–851, Jul. 2019.
- [23] D. Bhatia, W. Kim, S. Lee, S. W. Kim and D. Choi, “Tandem triboelectric nanogenerators for optimally scavenging mechanical energy with broadband vibration frequencies”, *Nano Energy*, vol. 33, 515–521, Mar. 2017.

[24] Y. Lee, S. H. Cha, Y.-W. Kim, K. Choi and J.-Y. Sun, “Transparent and attachable ionic communicators based on self-cleanable triboelectric nanogenerators”, *Nature Communications*, vol. 9, 1804, May 2018.

[25] W. Kim, H. J. Hwang, D. Bhatia, Y. Lee, J. M. Baik and D. Choi, “Kinematic design for high performance triboelectric nanogenerators with enhanced working frequency“, *Nano Energy*, vol. 21, 19-25, Mar. 2016.

[26] M. Seol, S. Kim, Y. Cho, K.-E. Byun, H. Kim, J. Kim, S. K. Kim, S.-W. Kim, H.-J. Shin and S. Park, “Triboelectric series of 2D layered materials”, *Advanced Materials*, vol. 30, 1801210, Aug. 2018.

[27] M. Kanik, M. G. Say, B. Daglar, A. F. Yavuz, M. H. Dolas, M. M. E.-Ashry and M. Bayindir, “A motion- and sound-activated, 3D-printed, chalcogenide-based triboelectric nanogenerator”, *Advanced Materials*, vol. 27, 2367-23769, Feb. 2015.

[28] R. Hinchet, W. Seung and S.-W. Kim, “Recent progress on flexible triboelectric nanogenerators for self-powered electronics, *ChemSusChem*, vol. 8, 2327-2344, Jul. 2015.

[29] Y. Zou, V. Raveendran and J. Chen, “Wearable triboelectric nanogenerators for biomechanical energy harvesting”, *Nano Energy*, vol. 77, 105303, Nov. 2020.

[30] H. J. Hwang, J. S. Kim, W. Kim, H. Park, D. Bhatia, E. Jee, Y. S. Chung, D. H. Kim and D. Choi, “An ultra-mechanosensitive visco-poroelastic polymer ion pump for continuous self-powered kinematic triboelectric nanogenerators”, *Advanced Energy Materials*, vol. 9, 1803786, Mar. 2019.

[31] J. S. Heo, J. Eom, Y.-H. Kim and S. K. Park, “Recent progress of textile-based wearable electronics: A comprehensive review of materials, devices, and applications”, *Small*, vol. 14, 1703034, Dec. 2017.

[32] W. A. D. M. Jayathilaka, K. Qi, Y. Qin, A. Chinnappan, W. S.-Garcia, C. Baskar, H. Wang, J. He and S. Cui, “Significance of nanomaterials in wearables: A review on wearable actuators and sensors”, *Advanced Materials*, vol. 31, 1805921, Dec. 2018.

[33] K. Venugopal, M. C. Valenti and R. W. Heath, “Device-to-device millimeter wave communications: Interference, coverage, rate, and finite topologies”, *IEEE Transactions on wireless communications*, vol. 15, 6175-6788, Sep. 2016.

[34] H. S. Kim, J.-H. Kim and J. Kim, “A review of piezoelectric energy harvesting based on vibration”, *International Journal of Precision Engineering and Manufacturing*, vol. 12, 1129-1141, Dec. 2011.

[35] S. Ulukus, A. Yener, E. Krkip, O. Simeone, M. Zorzi, P. Grover and K. Huang, “Energy harvesting wireless communications: A review of recent advances”, *IEEE Journal on Selected Areas in Communications*, vol. 33, 360-381, Mar. 2015.

[36] C. R. Bowen, H. A. Kim, P. M. Weaver and S. Dunn, “Piezoelectric and ferroelectric materials and structures for energy harvesting applications”, *Energy&Environmental Science*, vol. 7, 25-44, Nov. 2013.

[37] T. Yao, X. Guo, C. Li, H. Qi, H. Lin, L. Liu, Y. Dai, L. Qu, Z. Huang and P. Liu, “Highly sensitive capacitive flexible 3D-force tactile sensors for robotic grasping and manipulation”, *Journal of Physics D: Applied Physics*, vol. 53, 445109, Aug. 2020.

[38] J. Qiu, X. Guo, R. Chu, S. Wang, W. Zeng, L. Qu, Y. Zhao, F. Yan and G. Xing, “Rapid-response, low detection limit, and high-sensitivity capacitive flexible tactile sensor based on three-dimensional porous dielectric layer for wearable electronic skin”, *ACS Applied Materials&Interfaces*, vol. 11, 40716-40725, Oct. 2019.

- [39] Y.-M Choi, M. G. Lee and Y. Jeon, “Wearable biomechanical energy harvesting technologies”, *Energies*, vol. 10, 1483, Sep. 2017.
- [40] J. Zhao and Z. You, “A shoe-embedded piezoelectric energy harvester for wearable sensors”, *Sensors*, vol. 14, 12497-12510, Jul. 2014.
- [41] S.-H. Park, H. B. Lee, S. M. Yeon, J. Park and N. K. Lee, “Flexible and stretchable piezoelectric sensor with thickness-tunable configuration of electrospun nanofiber mat and elastomeric substrates”, *ACS Applied Materials&Interfaces*, vol. 8, 24773-24781, Aug. 2016.
- [42] J. Liu, Y. Jia, Q. Jiang, F. Jiang, C. Li, X. Wang, P. Liu, P. Liu, F. Hu, Y. Du and J. Xu, “Highly conductive hydrogel polymer fibers toward promising wearable thermoelectric energy harvesting”, *ACS Applied Materials&Interfaces*, vol. 10, 44033-44040, Dec. 2018.
- [43] M. Zadan, M. H. Malakooti and C. Majidi, “Soft and stretchable thermoelectric generators enabled by liquid metal elastomer composites”, *ACS Applied Materials&Interfaces*, vol. 12, 17921-17928, Mar. 2020.
- [44] G. Lee, C. S. Kim, S. Kim, Y. J. Kim, H. Choi and B. J. C, “Flexible heatsink based on a phase-change material for a wearable thermoelectric generator”, *Energy*, vol. 179, 12-18, Jul. 2019.
- [45] F. Wang, Z. Ren, J. Nie, J. Tian, Y. Ding and X. Chen, “Self-powered sensor based on bionic antennae arrays and triboelectric nanogenerator for identifying noncontact motions”, *Advanced Materials Technologies*, vol. 5, 1900789, Nov. 2019.
- [46] S. Li, W. Peng, J. Wang, L. Lin, Y. Zi, G. Zhang and Z. L. Wang, “All-elastomer-based triboelectric nanogenerator as a keyboard cover to harvest typing energy”, *ACS Nano*, vol. 10, 7973-7981, Aug. 2016.

[47] L. E. Helseth, “Interdigitated electrodes based on liquid metal encapsulated in elastomer as capacitive sensors and triboelectric nanogenerators”, *Nano Energy*, vol. 50, 266–272, Aug. 2018.

[48] Z. L. Wang, “On the first principle theory of nanogenerators from Maxwell’s equations”, *Nano Energy*, vol. 68, 104272, Feb. 2020.

[49] Q. Jiang, C. Wu, Z. Wang, A. C. Wang, J.-H. He, Z. L. Wang and H. N. Alshareef, “MXene electrochemical microsupercapacitor integrated with triboelectric nanogenerators as a wearable self-charging power unit”, *Nano Energy*, vol. 45, 266–272, Mar. 2018.

[50] X. Pu, M. Liu, X. Chen, J. Sun, C. Du, Y. Zhang, J. Zhai, W. Hu and Z. L. Wang, “Ultrastretchable, transparent triboelectric nanogenerators as electronic skin for biomechanical energy harvesting and tactile sensing”, *Science Advances*, vol. 3, e1700015, May 2017.

[51] T. Liu, M. Liu, S. Dou, J. Sun, Z. Cong, C. Jiang, C. Du, X. Pu, W. Hu and Z. L. Wang, “Triboelectric-nanogenerator-based soft energy-harvesting skin enabled by toughly bonded elastomer/hydrogel hybrids”, *ACS Nano*, vol. 12, 2818–2826, Mar. 2018.

[52] Z. Wu, T. Cheng and Z. L. Wang, “Self-powered sensors and systems based on nanogenerators”, *Sensors*, vol. 20, 2925, May 2020.

[53] Y.-C. Lai, J. Deng, S. L. Zhang, S. Niu, H. Guo and Z. L. Wang, “Single-thread-based wearable and highly stretchable triboelectric nanogenerators and their applications in cloth-based self-powered human-interactive and biomedical sensing”, *Advanced Functional Materials*, vol. 27, 1604462, Nov. 2016.

[54] X. Pu, L. Li, M. Liu, C. Jiang, C. Du, Z. Zhao, W. Hu and Z. L. Wang, “Wearable self-charging power textile based on flexible yarn supercapacitors and fabric nanogenerators”, *Advanced Materials*, vol. 28, 98–105, Nov. 2015.

- [55] X. Pu, L. Li, H. Song, C. Du, Z. Zhao, C. Jiang, G. Cao, W. Hu and Z. L. Wang, “A self-charging power unit by integration of a textile triboelectric nanogenerator and a flexible lithium-ion battery for wearable electronics”, *Advanced Materials*, vol. 27, 2472-2478, Mar. 2015.
- [56] S. Li, Q. Zhong, J. Zhong, X. Cheng, B. Wang, B. Hu and J. Zhou, “Cloth-based power shirt for wearable energy harvesting and clothes ornamentation”, *ACS Applied Materials&Interfaces*, vol. 7, 14912-14916, Jun. 2015.
- [57] J. Ge, L. Sun, F.-R. Zhang, Y. Zhang, L.-A. Shi, H.-Y. Zhao, H.-W. Zhu, H.-L. Jiang and S.-H. Yu, “A stretchable electronic fabric artificial skin with pressure-, lateral strain-, and flexion-sensitive properties”, *Advanced Materials*, vol. 28, 722-728, Nov. 2015.
- [58] Z. L. Wang, “Triboelectric nanogenerators as new energy technology and self-powered sensors - Principles, problems and perspectives”, *Faraday Discussions*, vol. 176, 447-458, Sep. 2014.
- [59] B. H. Kim, B. S. Barnhart and J. W. Kwon, “Electrostatic power generation using carbon-activated cotton thread on textile”, *Micro and Nano Systems Letters*, vol. 3, 3, Apr. 2015.
- [60] Y. Zhu, B. Yang, J. Liu, X. Wang, L. Wang, X. Chen and C. Yang, “A flexible and biocompatible triboelectric nanogenerator with tunable internal resistance for powering wearable devices”, *Scientific Reports*, vol. 6, 22233, Feb. 2016.
- [61] X. Wang, Y. Gu, Z. Xiong, Z. Cui and T. Zhang, “Silk-molded flexible, ultrasensitive, and highly stable electronic skin for monitoring human physiological signals”, *Advanced Materials*, vol. 26, 1336-1342, Dec. 2013.

- [62] T. Li, M. Liu, S. Dou, J. Sun, Z. Cong, C. Jiang, C. Du, X. Pu, W. Hu and Z. L. Wang, “Triboelectric-nanogenerator-based soft energy-harvesting skin enabled by toughly bonded elastomer/hydrogel hybrids” *ACS Nano*, vol. 12, 2818-2826, Mar. 2018.
- [63] G. Zhao, Y. Zhang, N. Shi, Z. Liu, X. Zhang, M. Wu, C. Pan, H. Liu, L. Li and Z. L. Wang, “Transparent and stretchable triboelectric nanogenerator for self-powered tactile sensing”, *Nano Energy*, vol. 59, 302-310, May 2019.
- [64] J. Zhu, X. Wang, Y. Xing and J. Li, “Highly stretchable all-rubber-based thread-shaped wearable electronics for human motion energy-harvesting and self-powered biomechanical tracking” *Nanoscale Research Letters*, vol. 14, 247, Jul. 2019.
- [65] R. Zhang, M. Hummelgard, J. Ortegren, M. Olsen, H. Andersson, Y. Yang and H. Olin, “Human body constituted triboelectric nanogenerators as energy harvester, code transmitters, and motion sensors”, *ACS Applied Energy Materials*, vol. 1, 2955-1960, May 2018.
- [66] C. Jacquemoud, K. B.-Garnier and M. Coret, “Methodology to determine failure characteristics of planar soft tissues using a dynamic tensile test”, *Journal of Biomechanics*, vol. 40, 468-475, Jan. 2007.
- [67] J. Park, D. Kim and Y. T. Kim, “Ultra-stretchable on-body-based soft triboelectric nanogenerator for electronic skin”, *Smart Materials and Structures*, vol. 29, 115031, Oct. 2020.
- [68] X. Chen, Y. Wu, J. Shao, T. Jiang, A. Yu, L. Xu and Z. L. Wang, “On-skin triboelectric nanogenerator and self-powered sensor with ultrathin thickness and high stretchability” *Small*, vol. 13, 1702929, Oct. 2017.

[69] N. Gogurla, B. Roy, J.-Y. Park and S. Kim, “Skin-contact actuated single-electrode protein triboelectric nanogenerator and strain sensor for biomechanical energy harvesting and motion sensing”, *Nano Energy*, vol. 62, 674-681, Aug. 2019.

[70] X. Yu, X. Liang, R. Krishnamoorthy, W. Jiang, L. Zhang, L. Ma, P. Zhu, Y. Hu, R. Sun and C.-P. Wong, “Transparent and flexible hybrid nanogenerator with welded silver nanowire networks as the electrodes for mechanical energy harvesting and physiological signal monitoring”, *Smart Materials and Structures*, vol. 29, 045040, Mar. 2020.

[71] K. Dong, Z. Wu, J. Deng, A. C. Wang, H. Zou, C. Chen, D. Hu, B. Gu, B. Sun and Z. L. Wang, “A stretchable yarn embedded triboelectric nanogenerator as electronic skin for biomechanical energy harvesting and multifunctional pressure sensing”, *Advanced Materials*, vol. 30, 1804944, Sep. 2018.

List of Publications

Paper

- 1) Jiwon Park, Daeun Kim and Youn Tae Kim, Soft and transparent triboelectric nanogenerator based E-skin for wearable energy harvesting and pressure sensing, *Nanotechnology*, 32, 385403 (2021)
- 2) Jiwon Park, Daeun Kim and Youn Tae Kim, Ultra-stretchable on-body-based soft triboelectric nanogenerator for electronic skin, *Smart Materials and Structures*, 29, 115031 (2020)
- 3) Dogyun Kim, Jiwon Park and Youn Tae Kim, Core-shell and helical-structured cylindrical triboelectric nanogenerator for wearable energy harvesting, *ACS Applied Energy Materials*, 2, 1357-1362 (2019)
- 4) Jiwon Park, Dogyun Kim, A Young Choi and Youn Tae Kim, Flexible single-strand fiber-based woven-structured triboelectric nanogenerator for self-powered electronics, *APL Materials*, 6, 101106 (2018)
- 5) Jiwon Park, A Young Choi, Chang Jun Lee, Dogyun Kim and Youn Tae Kim, Highly stretchable fiber-based single-electrode triboelectric nanogenerator for wearable devices, *RSC Advances*, 7, 54829-54834 (2017)
- 6) A Young Choi, Chang Jun Lee, Jiwon Park, Dogyun Kim and Youn Tae Kim, Corrugated textile based triboelectric generator for wearable energy harvesting, *Scientific Reports*, 7, 45583 (2017)

7) Chang Jun Lee, A Young Choi, Jiwon Park, Hyeon Jun Sim, Changsoon Choi, Seon Jeong Kim and Youn Tae Kim, Triboelectric generator for wearable devices fabricated using casting method, *RSC Advances*, 6, 10094-10098 (2016)

List of Publications

Conference

- 1) "Triboelectric nanogenerator based E-skin for wearable energy harvesting and pressure sensing", **J. Park**, D. Kim and Y. T. Kim, IEEE NANO, July 2021
- 2) "Foldable paper based triboelectric nanogenerator for green energy harvesting", D. Kim, **J. Park** and Y. T. Kim, IEEE NANO, July 2021
- 3) "On-skin based soft triboelectric nanogenerator for electronics skin", **J. Park**, D. Kim and Y. T. Kim, IEEE-NEMS, September 2020
- 4) "Flexible fiber based woven structured triboelectric nanogenerator for self-powered system", **J. Park**, D. Kim and Y. T. Kim, IEEE NANO, July 2018
- 5) "Helical structure-based triple cylindrical triboelectric nanogenerator", D. Kim, **J. Park** and Y. T. Kim, IEEE NANO, July 2018
- 6) "Highly stretchable fiber-based single-electrode triboelectric nanogenerator for wearable devices", **J. Park**, A. Y. Choi, C. J. Lee, D. Kim and Y. T. Kim, MRS Fall Meeting, November 2017
- 7) "Stretchable and flexible cylindrical-fiber-based triboelectric nanogenerator", D. Kim, A. Y. Choi, **J. Park**, C. J. Lee and Y. T. Kim, IEEE NANO, July 2017
- 8) "Flexible fiber-based triboelectric generator for self-powered sensors", **J. Park**, A. Y. Choi, C. J. Lee and Y. T. Kim, IEEE Sensors, October 2016

9) "Triboelectric generator made with corrugated stretchable textile for energy harvesting ", Y. S. Kim, J. Park, A Y. Choi and Y. T. Kim, MRS Fall Meeting, November 2015

10) "Flexible two-ply yarn based generator for energy harvesting", J. Park, Y. S. Kim, C. J. Lee and Y. T. Kim, MRS Fall Meeting, November 2015

List of Publications

Patent

- 1) Youn Tae Kim, Jiwon Park, Daeun Kim, "Body attachable triboelectric generating device and manufacturing method thereof", US Application Number: 17/534,044, 2021
- 2) Youn Tae Kim, Jiwon Park, Daeun Kim, "Apparatus for transmitting power wirelessly using capacitive coupling", US Application Number: 17/534,117, 2021
- 3) 김윤태, 박지원, 김다운, "신체 부착형 마찰전기 발전소자 및 이의 제조 방법", KR Application Number: 10-2021-0127983, 2021
- 4) 김윤태, 박지원, 김다운, "용량성 결합을 이용한 무선 전력 전송 장치", KR Application Number: 10-2021-0063759, 2021
- 5) Youn Tae Kim, Jong Jin Baek, Jiwon Park, Mingu Kang "Capsule-type endoscope capable of two-way communication", US Application Number: 17/117,956, 2020
- 6) 김윤태, 박지원, 최아영, 김도균, "섬유형 마찰전기 발전 소자, 이를 이용하여 직조된 직물 및 섬유형 마찰전기 발전 소자의 제조 방법", KR Registration Number: 10-2140939, 2020
- 7) Youn Tae Kim, A Young Choi, Chang Jun Lee, Jiwon Park, Dogyun Kim "Fibrous energy harvesting device having corrugated structure and wearable item including the same", US Registration Number: 10/680,536, 2020

8) 김윤태, 백종진, **박지원**, 강민구 "양방향 통신이 가능한 캡슐형 내시경", KR Application Number: 10-2019-0164955, 2019

9) 김윤태, 최아영, 이창준, **박지원**, 김도균 "주름 구조를 가진 섬유형 에너지 하베스팅 소자 및 이를 포함하는 의류", KR Registration Number: 10-1839301, 2018

10) 김윤태, 이창준, 최아영, **박지원**, 김도균 "웨어러블 에너지 발생장치", KR Registration Number: 10-1796185, 2017

11) Youn Tae Kim, Chang Jun Lee, A Young Choi, **Jiwon Park**, Dogyun Kim, "Wearable energy generating apparatus", US Registration Number: 15/368,807, 2016

ABSTRACT

Development of Woven Structured and Skin-attachable Nanogenerator for Wearable Energy Harvesting

Jiwon Park

Advisor: Prof. Youn Tae Kim, Ph.D.

**Department of IT Fusion Technology,
Graduate School of Chosun University**

Recently, wearable energy harvesting technology has been attracting attention to solve the power supply problem in wearable systems, such as smart clothing and E-skin. This study proposes a nanogenerator that can be worn comfortably by a human being. It can harvest energy through human movements and can be applied in various fields. In particular, methods for securing durability and flexibility and improving efficient power generation performance, which are core requirements of wearable energy harvesting devices, were presented. We developed fiber, woven-structured, body-attachable, and E-skin-based nanogenerators and analyzed the effects of each parameter by measuring the physical and electrical properties of the nanogenerators. Stretchability and durability were secured through a composite of polymer elastomers and conductive yarns, and the charge density was increased by patterning the surface of the triboelectric material through a simple and efficient casting method. Consequently, the nanogenerators demonstrated an elasticity $\geq 100\%$, excellent durability over 5000 operating cycles, and power generation of up to 154 mW/m^2 to operate electronic

devices. In addition, in the case of the E-skin type, bio-signals were measured by applying an integrated pressure sensor; moreover, energy harvesting was possible owing to body movements. The developed nanogenerator can supply power to wearable systems and is expected to be used in applications such as electronic textiles, flexible electronic devices, human-machine interfaces, and bio-monitoring.

Acknowledgement

I would like to thank my advisor, Professor Youn Tae Kim for his supervision, understanding, support, encouragement and personal guidance as I was working on this research and the thesis. I am deeply grateful to all the professors from whom I have learned a great deal of knowledge.

In addition, I have the deepest appreciation for the constructive criticism and excellent advice that provided by Prof. Sung Bum Pan, Prof. Hyun-Sik Choi, Prof. Myung-Ae Chung and Prof. Seon Jeong Kim and during the preparation of my thesis, as well as for their detailed review of the thesis after it was completed.

During this work, I collaborated with all my colleagues in the laboratory and I have great regard for all of them and wish to extend my sincerest thanks to all those in the Department of IT Fusion Technology who helped as I conducted my work.

My deepest thanks go to my family for all the care and support he has given me over many years. You are the best family in the world.

January 2022

Jiwon Park